

1 Papillomavirus can be transmitted through the blood and produce infections in
2 blood recipients: Evidence from two animal models

3
4 #^{1,2} Nancy M. Cladel, #^{3,4} Pengfei Jiang, ^{1,2} Jingwei J. Li, ⁵Xuwen Peng, ⁶Timothy K. Cooper, ³
5 Vladimir Majerciak, ^{1,2} Karla K. Balogh, ^{7,8}Thomas J. Meyer, ^{1,2} Sarah A. Brendle, ^{1,2} Lynn R.
6 Budgeon, ^{1,2}Debra A. Shearer, ⁵Regina Munden, ⁷Maggie Cam, ⁹Raghavan Vallur, ^{1,2,9} Neil D.
7 Christensen, ^{*3}Zhi-Ming Zheng, and ^{*1,2}Jiafen Hu
8 # Equal contributions to this work as a first author
9

10 ¹The Jake Gittlen Laboratories for Cancer Research, Pennsylvania State University College of
11 Medicine, Hershey, PA 17033, USA; ²Department of Pathology, Pennsylvania State University
12 College of Medicine, Hershey, PA 17033, USA; ³Tumor Virus RNA Biology Section, RNA
13 Biology Laboratory, National Cancer Institute, NIH, Frederick, MD 21702, USA; ⁴ Department
14 of Immunology and Microbiology, School of Basic Medical Sciences, Wenzhou Medical
15 University, Wenzhou 325035, Zhejiang, P. R. China; ⁵Department of Comparative Medicine,
16 Pennsylvania State University College of Medicine, Hershey, PA 17033, USA; ⁶Integrated
17 Research Facility at Fort Detrick, National Institute of Allergy and Infectious Diseases, NIH,
18 Fort Detrick, Frederick, MD, 21702, USA; ⁷CCR Collaborative Bioinformatics Resource
19 (CCBR), Center for Cancer Research, NCI, NIH, Bethesda, MD 20814, USA; ⁸Advanced
20 Biomedical Computational Science, Frederick National Laboratory for Cancer Research,
21 Frederick, MD 21702, USA; ⁹Department of Microbiology and Immunology, Pennsylvania State
22 University College of Medicine, Hershey, PA 17033, USA,

23 Corresponding authors:

24 Jiafen Hu (fjh4@psu.edu, 7175314700)

25 Zhi-Ming Zheng (zhengt@exchange.nih.gov, 301-846-7634);

26 **Running title:** Papillomavirus can be transmitted through blood

27 **Keywords:** Papillomavirus, blood transfusion, animal models, CRPV/rabbit model,

28 MmuPV1/mouse model, viral infection

29 **SUMMARY**

30 Human papillomaviruses cause 5% of human cancers. Currently, blood banks do not
31 screen for these viruses. We demonstrate that blood transfused from papillomavirus-infected
32 animals produces infections in recipients. Public health implications are significant if the same is
33 true for humans.

34

35 **Abbreviations:**

36 **HPV:** Human Papillomavirus

37 **CRPV:** The Cottontail Rabbit Papillomavirus

38 **MmuPV1:** The Mouse Papillomavirus

39 **NZW:** New Zealand White

40 **IV:** Intravenous

41 **PBMCs:** Peripheral Blood Mononuclear Cells

42 **PCA:** Principle Component Analysis

43 **HCT:** Hematopoietic Cell Transplantation

44

45 **Definitions**

46 **Local papillomavirus infection:** An infection initiated by the direct application of virus or viral
47 DNA to the site of infection

48 **Intravenous (IV) papillomavirus infection:** An infection resulting from blood-borne delivery
49 of virus or viral DNA to the site of infection.

50

51

52 **ABSTRACT**

53 Human papillomavirus (HPV) infections are commonly thought to be strictly sexually
54 transmitted. However, studies have demonstrated the presence of HPV in cancers of many non-
55 sexual internal organs, raising the question as to how the viruses gain access to these sites. A
56 possible connection between blood transfusion and HPV-associated disease has not received
57 much attention. We show, in two animal models, that blood infected with papillomavirus yields
58 infections at permissive sites. Furthermore, we demonstrate that blood from actively infected
59 mice can transmit the infection to naïve animals. Finally, we report papillomavirus infections in
60 the stomach tissues of animals infected via the blood. Stomach tissues are not known to be
61 permissive for papillomavirus infection, although the literature suggests that HPVs may be
62 associated with a subset of gastric cancers. These results indicate that the human blood supply,
63 which is not screened for papillomaviruses, could be a potential source of HPV infection and
64 subsequent cancers.

65

66

67

68

69

70

71

72

73

74

75 INTRODUCTION

76 This study grew out of an observation made in 2005 (Bodaghi et al., 2005a) that a subset
77 of children with HIV also had detectable levels of human papillomavirus (HPV) in their
78 peripheral blood mononuclear cells (PBMCs). Some of these children were hemophiliacs who
79 had contracted HIV through contaminated blood. All were reported to be sexually naïve.
80 Importantly, HPV was detected in three out of the 19 seemingly healthy blood donors. A later
81 study in 2009 demonstrated that HPV DNA is present in about 8.3% of healthy donor PBMCs in
82 Australia (Chen et al., 2009). In addition, HPV has been detected in many malignant tissues,
83 including the head and neck (Taberna et al., 2017), esophagus (Agalliu et al., 2018), lung
84 (Shikova et al., 2017), colorectum (Bodaghi et al., 2005b) (Baandrup et al., 2014), prostate
85 (Glenn et al., 2017; Tachezy et al., 2012), breast (ElAmrani et al., 2018; Malhone et al., 2018)
86 and stomach (Mirzaei et al., 2018; Zeng et al., 2016). We asked the following questions: 1)
87 Could blood be a non-sexual mode for the transmission of papillomavirus infections? 2) As the
88 blood bank does not currently screen for the presence of HPV, is the public being put at risk by
89 this omission?

90 HPV is strictly species-specific (Martinez and Troconis, 2014). Thus, it is not possible to
91 study HPV infections directly in any animals. However, our laboratory is fortunate to have two
92 preclinical animal models with their own naturally occurring papillomaviruses (Christensen et
93 al., 2017; Doorbar, 2016; Hu et al., 2017; Uberoi and Lambert, 2017). We have developed
94 methods that allow us to use these models to test the possibility of papillomavirus transmission
95 by blood.

96 The Cottontail Rabbit Papillomavirus (CRPV) infection model has been in use in our
97 laboratory for more than three decades. CRPV infections produce cutaneous tumors, which, in

98 time, progress to cancer (Christensen et al., 2017). Our first series of studies for the current
99 project was completed with this model: 1) We detected viral DNA in the blood of CRPV infected
100 animals; 2) We infected domestic rabbits with either infectious virions or viral DNA, via the
101 marginal ear vein, and observed tumor growth at pre-wounded back sites; 3) We drew blood
102 from two animals that had received CRPV virions intravenously and then transfused that blood
103 into two naïve animals via the marginal ear vein. Within ten weeks, a lesion appeared at the back
104 of one of two tested recipients. These results demonstrate that blood containing active
105 papillomavirus could transmit the virus to the wounded epithelium of a naïve host via the
106 circulatory system. *These early studies confirmed the possibility that papillomaviruses can*
107 *indeed be transmitted by blood and give rise to infections at receptive sites in naïve hosts.*

108 Next, we extended these studies to the mouse papillomavirus (MmuPV1) model, which
109 has been under development over the past seven years in our and other laboratories (Hu et al.,
110 2017; Uberoi and Lambert, 2017). MmuPV1 is the first mouse papillomavirus suitable for large-
111 scale laboratory studies and has been proven to be highly malleable in our hands. We have
112 shown that MmuPV1 has both cutaneous and mucosal tropisms (Cladel et al., 2017a; Cladel et
113 al., 2017b; Cladel et al., 2013). For this study, we carried out two experiments with these mice.
114 1) Naïve animals were infected with infectious virions via the tail vein. As in the case of the
115 rabbit model, infections developed at susceptible sites (both cutaneous and mucosal sites) in
116 these intravenously infected mice. *Furthermore, active infections were detected in the stomachs*
117 *of three of the tested animals.* 2) Blood was drawn from infected mice about seven month post
118 infection and transfused into naïve animals. Once again, infections developed at medically
119 relevant cutaneous and mucosal sites in the naïve animals. These sites included the mucosa of the
120 vagina, penis, oral cavity and anus, as well as cutaneous tail and muzzle sites. Furthermore,

121 active *infections were detected in the stomach of one of the tested animals*. These results are
122 provocative and provide direct evidence of blood transmission of papillomavirus from an
123 infected animal to a naïve animal. Our findings consequently call into question the safety of
124 human blood supplies. They raise the question “Should donor blood be routinely screened for the
125 presence of HPVs before being distributed to patients?”

126

127 **RESULTS**

128 *Intravenous (IV) delivery of CRPV virions replicates the patterns observed with skin*
129 *infections.*

130 If papillomavirus infections are capable of being transmitted via the blood, that implies
131 the infectious agents are able to survive in the blood. We first applied the rabbit model to test
132 whether CRPV virus deliberately introduced into the blood stream could yield infections at
133 prewounded skin sites. Two outbred NZW rabbits (NZW#1 and NZW#2) and one HLA-A2.1
134 transgenic rabbit were used in this pilot study. Each animal was infected via the marginal ear
135 vein with CRPV virions (500 μ l of the viral stock= 2.75×10^{10} viral DNA equivalents)
136 (Supplementary Table 1). The amount of virus in the circulation was estimated to be 1.8×10^5
137 copies/ μ l blood. This figure is based on an estimated blood volume of 150 ml per animal. On
138 each animal, eight back skin sites had been wounded three days prior to introduction of virus as
139 per our local skin infection protocol (Cladel et al., 2008). The pre-wounded sites were scratched
140 with a 28-gauge needle (Cladel et al., 2008) following intravenous (IV) viral infection and then
141 monitored for tumor growth. Four weeks post infection, tumors were visible at the wounded sites
142 of all three animals, and the tumors increased in size over time during the first six weeks post
143 infection (Fig. 1 A-C). The tumor growth pattern mimicked the patterns observed in local skin

144 infections in our previous studies (Hu et al., 2007b). Tumors in the transgenic animal (Fig. 1 C)
145 regressed over time, as has often been observed in these animals with local skin infections (Hu et
146 al., 2007b). Tumors on NZW#1 persisted as shown in Fig. 1 D. Interestingly, no tumors
147 developed at the marginal ear vein sites , which further confirms previous findings that
148 prewounding is crucial for viral infection in our CRPV/rabbit model (Cladel et al., 2008).

149 The experiment was repeated using five-fold fewer virions (3.6×10^4 / μ l blood) to infect
150 four naïve NZW rabbits (NZW#3-6) intravenously. In addition to eight prewounded sites, two
151 back skin sites on each animal were wounded only on the day of IV infection. 18 out of 32 pre-
152 wounded sites developed papillomas, whereas none of the eight sites wounded on the day of IV
153 infection developed papillomas ($P < 0.05$, Fisher's exact test). These results recapitulate our
154 findings for local skin infections (Fig. 1 F) and lend further support for the role of wound healing
155 in the development of papillomavirus infections (Cladel et al., 2008). Again, no lesion was found
156 at any IV injection sites on these rabbits.

157 We further compared the tumors induced by IV infection and those induced by local skin
158 infection by histological analysis. Representative tumors from each of two IV infection
159 experiments (Fig. 1 G and I, 20 \times) are shown. Histology similar to that seen in local skin
160 infection (Fig. 1 K, 20 \times) is observed by H&E staining. Viral presence was detected by in situ
161 hybridization (Fig. 1 H and J, 20 \times arrows) and is similar to that found in the rabbits with local
162 skin infection (Fig. 1 L, 20 \times arrows).

163 Anti-CRPV antibodies were detected in the sera of all intravenously infected animals, but
164 antibody level did not correlate with tumor size (Fig. 2 A). These antibodies were also
165 neutralizing in our in vitro neutralization assays (Fig. 2 B). Collectively, these findings prove
166 that CRPV circulating in the blood of rabbits can initiate infection at prewounded cutaneous sites,

167 the preferred sites for CRPV infection, and stimulate anti-viral immune responses in these rabbits
168 just as found in local skin infected animals (Hu et al., 2007a).

169
170 ***RNA sequencing (RNA-seq) analysis demonstrated similar CRPV transcription patterns for all***
171 ***cutaneous tumors resulting from either local skin infections or intravenous CRPV infections.***

172 To analyze CRPV transcripts arising from the tumors generated by CRPV virions
173 through marginal ear vein injection, total RNA was isolated from four tumors from four different
174 animals, depleted of ribosomal RNA and analyzed by RNA-seq. By mapping the RNA-seq raw
175 reads to the newly arranged linear CRPV genome starting from nt 7421 and ending at nt 7420
176 using RNA sequence aligner TopHat, we obtained 18318, 24014, 62100, and 128869 viral reads
177 for the respective tumor tissues. These reads account for 0.0290%, 0.0442%, 0.0911%, and
178 0.1960% of total RNA reads obtained from these samples. By uploading these uniquely mapped
179 viral RNA reads to the Integrative Genomics Viewer (IGV) program to visualize reads coverage
180 profile in parallel with the CRPV genome, we found three major coverage peaks in the E6, E7
181 and E1^{E4} regions among all tumor tissues (Fig. 3).

182 RNA-seq data of three groups of ten examined tissues (four normal skin tissues and three
183 tumor tissues each induced by IV infection or local skin infection) were further analyzed by
184 Principle component analysis (PCA). A well grouped dataset was found (Fig. 4 A). Interestingly,
185 one of three tumors derived from IV infections had high virus titer by RNA-seq raw reads (Fig.
186 3) and the altered gene expression pattern was close to that of the tumors induced by local skin
187 infection (Fig. 4 A). Volcano plots of 17742 annotated genes in the rabbit genome exhibited
188 significant differences in the host transcriptome of the normal control skin group compared with
189 the tumor groups induced either by IV infection or local skin infection (Fig. 4 B-C). The

190 dysregulated expression of the genes is detailed in supplemental Table 3. Approximately 3,000
191 out of 5,224 genes were similarly dysregulated by the two routes of CRPV infections (Fig. 4 D).
192 Overall, fewer genes (3,485) displayed the altered expression in IV infected tumors when
193 compared with those in locally skin-infected tumors (4,799) (Fig. 4 D). Using the thresholds of
194 $P \leq 0.05$ and absolute fold change (FC) ≥ 2.0 of differentiated gene expression, we analyzed the
195 top 100 up-regulated and top 100 down-regulated genes in each experimental group (Fig. 4 F) by
196 heatmap analysis and identified the most important genes with differential expression common in
197 the tumors derived from both routes of virus infections (Fig. 4 E), notably the genes with
198 upregulated expression. For the genes with reduced expression, five expression patterns could be
199 subgrouped according to their reduced expression levels, with the expression of only a few genes
200 being commonly downregulated in the tumors derived from both infection routes. A majority of
201 them exhibited the expression reduction from cutaneous infection low to IV infection high or
202 vice versa (Fig. 4 E). Based on gene function and its RNA abundance, we subsequently verified
203 nine rabbit genes with significantly different expression in CRPV-induced tumors from both
204 infection routes by real-time qPCR (Table 1) (Fig. 5 A-B). Consistent with RNA-seq data, the
205 expression of SLN, TAC1, MYH8, and PGAM2 were down-regulated, whereas SDRC7,
206 KRT16, S100A9, IL36G, and FABP9 were all up-regulated in both blood (Animal #9, #11, and
207 #12) and skin (Animal #6, #7, and #8)-induced tumors when compared to those in normal skin of
208 control animals (Fig. 5 B). Consistent with the RNA-seq results, western blot analysis of two
209 selected genes further confirmed the increased protein expression of S100A9 and decreased
210 expression of APOBEC2 in tumors induced by both routes of infections (Fig. 5 C). Taken
211 together, these findings strongly support the hypothesis that bloodborne and local skin
212 papillomavirus infections have similar infectivity mechanisms.

213 ***CRPV DNA delivered intravenously induced tumors at prewounded sites and replicated the***
214 ***pattern previously observed with DNA locally delivered to pre-wounded sites.***

215 CRPV DNA delivered locally to wounded sites results in tumor growth (Cladel et al.,
216 2008; Hu et al., 2002; Kreider et al., 1995). HPV DNA can be detected in human blood (Bodaghi
217 et al., 2005a; Chen et al., 2009; Cocuzza et al., 2017; Jeannot et al., 2016). We hypothesized that
218 the rabbit model could be used to determine if viral DNA in the blood could pose a potential risk
219 for infection. Our previous work determined that about 1.3×10^{10} viral DNA equivalents would be
220 needed to guarantee tumor growth in all skin sites locally treated with viral DNA, and that a dose
221 as low as 1.3×10^9 viral DNA equivalents would be capable of inducing tumors at a subset of sites
222 (Supplementary Table 2). To accommodate for dilution as well as possible degradation of DNA
223 in the circulatory system, we inoculated 500 μg of viral DNA (estimated to be 4.6×10^{11} copies
224 / μl blood) into the ear veins of two rabbits with pre-wounded skin sites on the backs. Both
225 rabbits grew tumors at these pre-wounded skin sites at week nine post IV infection. Histology
226 (Fig. 6 B) of one representative papilloma (Fig. 6 A) was similar to that of the tumors initiated by
227 local skin infections by virions (Fig. 1 K) with typical epithelial koilocytes in the infected area.

228
229 ***Transfusion of blood containing CRPV virus resulted in tumors at prewounded back sites.***

230 The driving question behind our research was “Can transfusion of human blood
231 containing HPV sequences result in papillomavirus infection in the recipient?” This question
232 cannot be answered with experiments using human subjects, but it can be approached using
233 animal models. In a small pilot study designed to provide proof of principle data, two outbred
234 NZW domestic rabbits were intravenously infected with CRPV virions (1.8×10^5 copies/ μl
235 blood). Twenty-five minutes after the virus inoculation, 10 mL of blood was withdrawn from

236 each donor rabbit and infused into corresponding siblings, each with eight pre-wounded back
237 skin sites. Viral concentration was estimated to be 1.3×10^4 copies/ μ l of blood. One recipient
238 grew a skin tumor ten weeks after receiving blood from the donor (Fig. 7 A). Histology of this
239 tumor (Fig. 7 B) is similar to that shown in Fig. 1K. Viral DNA was detected in the tumor by in
240 situ hybridization (Fig. 7 C, 60 \times). No tumors were detected at the sites that had not been pre-
241 wounded.

242

243 ***Athymic mice inoculated intravenously with MmuPV1 developed infections at both cutaneous***
244 ***and mucosal tissues.***

245 Following the demonstration that CRPV delivered intravenously could yield infections
246 and tumor formation at prewounded skin sites, we next wished to determine whether the same
247 would be true for athymic nude mice in which MmuPV1 infects both mucosal and cutaneous
248 tissues (Hu et al., 2017). We were also interested in a possible sex bias during MmuPV1
249 infection. To explore this possibility, this experiment was conducted using equal numbers of
250 male and female animals.

251 1×10^8 viral DNA equivalent virions were carefully injected into the tail vein of six female
252 (Fig. 8 A) and six male (Fig. 8 B) Hsd: NU mice that had been pre-wounded at both cutaneous
253 and mucosal sites according to our standard protocol (Cladel et al., 2013; Hu et al., 2015). The
254 injection tail vein sites were treated topically with an excess dose of neutralizing monoclonal
255 antibody (MPV.A4) immediately post injection to neutralize any virions remaining at the site
256 (Supplementary Figure 1) (Cladel et al., 2017b). The animals were monitored for tumor growth
257 at the prewounded cutaneous sites and for viral DNA by qPCR at mucosal sites (Hu et al., 2015).
258 All tails of the infected mice grew tumors at the prewounded sites (representative mouse from

259 female and male groups respectively, Fig. 8 A, B). No tumors developed at the sites of injection
260 during the first ten weeks, indicating MPV.A4 efficiently blocked any possible skin
261 contamination during tail IV injection. Mucosal sites (the oral cavity, anus, vagina, and penis)
262 were positive for viral DNA by qPCR (Hu et al., 2015), as well as by immunohistochemistry and
263 in situ hybridization (ISH) (Fig. 8 C).

264

265 ***Active infections were found in stomach tissues of mice infected via tail vein injection with***
266 ***MmuPVI.***

267 In view of the many observations in the literature that papillomavirus sequences can
268 sometimes be found in cancers of internal organs, we examined whether blood-borne infections
269 could result in internal organ infections. The organs of selected intravenously infected mice were
270 examined for tissue pathological changes by H&E staining; for viral DNA by in situ
271 hybridization; and for viral capsid protein L1 by immunohistochemistry. Interestingly, the non-
272 granular stomach tissues of three out of eleven intravenously infected mice were found to be
273 positive for both viral DNA and L1 protein (Fig. 9). One of the three stomach tissues showed a
274 focally extensive plaque lesion of mild to moderate hyperplasia with atypia (Fig. 9 A). Abundant
275 hyperkeratosis with what appeared to be crypt formation was also found. There were occasional
276 positive nuclei within the stratum spinosum and granulosum with abundant positive staining of
277 both viral DNA and viral L1 protein in the cornified layers. There were multifocal cytoplasmic
278 hybridization signals with parietal cells in the glandular stomach. Two stomach tissues displayed
279 a small isolated (possibly pedunculated) focus of mild hyperplasia with cytological and nuclear
280 atypia (low grade) in the non-glandular stomach with scattered individual nuclear positive cells
281 (Fig. 9 D). These tissues were positive for both viral DNA, shown by in situ hybridization (Fig. 9
282 B and E, 20×, in blue), and for viral capsid protein, shown by immunohistochemistry (Fig. 9 C

283 and F, 20×, in red). No other organs were found to be positive for MmuPV1 in the examined
284 animals. This observation indicates that mouse tissues not normally permissive for MmuPV1
285 infection can become infected when the route of viral delivery is via the blood.

286

287 ***Transfusion of naïve mice with blood from mice with active infections yielded tumors at***
288 ***prewounded sites.***

289 Since the impetus for this study was the concern that papillomaviruses might be spread
290 from an infected to an uninfected individual via the blood, we next examined the ability of mice
291 with active infections to transmit the infection to naïve animals via blood transfusion. Two
292 infected mice (one male and one female) were sacrificed at seven months after initial IV
293 infection and 0.2 ml of blood from each animal was transfused via tail vein injection into three
294 male (M1-M3) and three female (F1-F3) naïve littermates. The injection tail vein sites were
295 treated topically with an excess dose of neutralizing monoclonal antibody (MPV.A4)
296 immediately post injection to neutralize any virions remaining at the site (Cladel et al., 2017b).
297 The corresponding recipients had been pre-wounded according to our usual protocol (Cladel et
298 al., 2017a). At ten weeks post infection, all recipients, both male and female, were positive for
299 viral infection and tumor growth at all of the wounded sites (Fig. 10 A-D). No lesions developed
300 at the sites of injection. The tissues were positive for viral DNA (Fig. 10E). *Importantly, one*
301 *stomach tissue was found to be positive for viral DNA (ISH, 60×, in blue) and capsid protein*
302 *(IHC, arrows, 60×, in red, Fig. 10 F).* These findings conclusively demonstrate that blood from
303 animals with papillomavirus infections can in fact transmit infections to naïve animals,
304 especially those that are immunosuppressed. Furthermore, the stomach can become infected
305 under these conditions.

306 *Viral DNA was detected in blood samples of CRPV infected rabbits and MmuPV1 infected*
307 *athymic mice.*

308 If blood transmission is one route of papillomavirus dissemination, then there should be a
309 DNA signature in the blood of infected animals. PCR amplification, rolling circle amplification
310 and DNA sequencing were performed to evaluate the presence of CRPV or MmuPV1 DNA in
311 the blood of both locally and IV infected rabbits and athymic mice respectively. Viral DNA was
312 detected in the whole blood of both CRPV-infected rabbits (12 /29) and MmuPV1-infected mice
313 (8/12) which were used in our previous studies (Cladel et al., 2008). 12 out of 31 mouse serum
314 samples also tested positive for the presence of viral sequences but none of the rabbit sera were
315 positive. These findings suggest the possibility that systemic papillomavirus infections might
316 have been established for much longer periods in the immunodeficient mice when compared
317 with the immunocompetent rabbits. Consistent with these findings, a systemic infection has also
318 been reported in bovine papillomavirus (BPV)-infected animals (Sadeghi et al., 2017).

319

320 **DISCUSSION**

321 In this study we examine the significance of papillomavirus infection in the blood. If
322 papillomaviruses can, indeed, be transmitted via the blood, millions of patients could be at risk of
323 HPV infections (Laffort et al., 2004; Shanis et al., 2018). Blood is routinely screened for human
324 immunodeficiency virus (HIV), hepatitis C (HCV), and hepatitis B (HBV). Procedures are being
325 developed to detect emerging viruses such as Dengue and Zika (Stramer, 2014). However, there
326 is no screening for HPVs. This omission appears to stem from the assumption that HPV-
327 associated human cancers, primarily cervical cancer, are strictly sexually transmitted (Khoury et
328 al., 2018). While that is true in many cases, it does not explain the finding that HPV can be

329 detected in the blood of a subset of sexually naïve children with hemophilia who have received
330 multiple transfusions (Bodaghi et al., 2005a). Nor does it explain the occasional presence of
331 HPV sequences in tumors of organs not normally exposed to the virus via sex, such as the
332 stomach, prostate, breast, colon, bladder, esophagus, and lung (Agalliu et al., 2018; Akhtar and
333 Bansal, 2017; Damin et al., 2007; Malhone et al., 2018; Mirzaei et al., 2018; Russo et al., 2018;
334 Salyakina and Tsinoremas, 2013; Shigehara et al., 2014). We asked whether such observations
335 could be due to transmission of the virus through the blood.

336 All papillomaviruses are highly species specific. Therefore a human papillomavirus
337 cannot infect any animal (Campo, 2002). As a result, studies of these viruses have historically
338 been undertaken using animal models (Christensen et al., 2017). These include Cottontail Rabbit
339 Papillomavirus (CRPV) and mouse papillomavirus (MmuPV1) (Ingle et al., 2011). Our
340 laboratory has done much pioneering work with the CRPV/rabbit model and the
341 MmuPV1/mouse model (Christensen et al., 2017; Hu et al., 2017). The domestic rabbit
342 (*Oryctolagus cuniculus*) is not the natural host for CRPV. CRPV was isolated from its natural
343 host, the wild cottontail rabbit of the Western United States (*Sylvilagus floridanus*) (Escudero
344 Duch et al., 2015). While the tumors in both animals are similar in appearance, the cottontail
345 rabbit produces far more virus than does the domestic rabbit (Christensen et al., 2017).
346 Intriguingly, these tumors are highly localized and cross contamination has never been seen in
347 our domestic rabbit CRPV studies. The MmuPV1 mouse model has been recently established
348 and immunocompromised mice are most susceptible to MmuPV1. MmuPV1 secondary
349 infections are common although secondary infections always appear much later than the primary
350 infections (Cladel et al., 2017b; Cladel et al., 2013; Hu et al., 2015). By using a neutralizing
351 monoclonal antibody MPV.A4 that completely neutralized both cutaneous and mucosal

352 MmuPV1 infections when the athymic mice were passively immunized (supplementary Figure
353 1), we demonstrated that an excess of this antibody, immediately applied to the tail vein injection
354 site after infusion with MmuPV1, could prevent contamination from IV infection. No tumors at
355 these injection sites were ever observed.

356 Armed with the CRPV and MmuPV1 preclinical models, we determined to address the
357 question of transmissibility of papillomaviruses through the blood. We demonstrated that 1)
358 Viral sequences could be detected in the blood of infected animals; 2) Virus introduced into the
359 blood could yield tumors at receptive sites, both cutaneous and mucosal; 3) CRPV DNA
360 introduced into the blood stream yielded papillomas at prepared skin sites; 4) Similar
361 mechanisms are used for infections via the blood and by direct application of virus to the skin as
362 determined by RNA-seq analysis; 5) Transfusion of blood from an animal that had received virus
363 via intravenous infection to a naïve sibling resulted in papillomas in the transfusion recipient; 6)
364 Virus introduced via intravenous delivery not only resulted in infections at the expected sites but
365 also at sites that are not normally permissive for MmuPV1 infections, and 7) Blood from animals
366 with active infections could induce infections in naive mice when transfused into these animals.

367 We conducted RNA-seq analysis to compare the transcriptomes of CRPV tumors induced
368 by local skin infection or IV infection. To allow for viral dilution in the blood during IV
369 infection a 10,000 fold excess of virus was used relative to that used for local infection. Despite
370 the possibility of stimulating host immune responses (Christensen et al., 1996), these IV
371 infections induced tumor growth at the prewounded back skin sites. Interestingly, the total
372 percentage of viral transcripts was much lower in tumors induced intravenously relative to
373 tumors induced locally. This is most likely because only a small portion of the IV inoculated
374 virus particles could reach the susceptible skin sites through the circulation. However, the

375 patterns of viral transcription in the tumors were identical for both routes of infections. We
376 further analyzed the host gene transcriptome of tumors resulting from both infection routes.
377 Consistent with findings for the viral RNA reads, we found dysregulated expression of fewer
378 genes in IV infection-induced tumors than in local infection-induced tumors. Although these two
379 different infection routes induced different numbers of genes with altered expression, we found
380 that the majority of the genes with significantly different expression were common to all tumors
381 examined by RNA-seq. A subset of those with altered expression was selectively verified by RT-
382 qPCR and Western blotting. These data provide further evidence that mechanisms for
383 papillomavirus IV infection and local infection are similar.

384 Most individuals acquire papillomavirus infections at some point in their lifetimes
385 (Gravitt and Winer, 2017). These infections are generally asymptomatic and the individual may
386 not even know he or she is infected. Sexually transmitted infections are very common in young
387 people, a cohort commonly represented in the pool of blood donors. Most papillomavirus
388 infections are thought to clear spontaneously but the process often occurs over a lengthy time
389 period of 1-2 years or more (Shew et al., 2015). In 10-20% of that HPV infected population,
390 infection with the same viral species reappears at a later date (Martinez and Troconis, 2014).
391 This supports the concept of latency as an alternative to clearance (Gravitt, 2011; Gravitt, 2012;
392 Gravitt and Winer, 2017). In a small percentage of infected people, the viral infection does not
393 clear at all and eventually progresses to cancer. Papillomaviruses are almost always implicated in
394 cervical cancer, a leading cause of death in women of child bearing age in the developing world
395 (Serrano et al., 2017).

396 Papillomaviruses are being identified in an increasing number of oral cancers, one of the
397 malignancies that is rapidly escalating worldwide (Taberna et al., 2017). For reasons that are still

398 unclear, the immune system is not capable of eradicating a subset of infections. It is possible that
399 virus from acute or latent infections makes its way, in some yet to be determined manner, into
400 the blood stream (Moustafa et al., 2017). Our results from animal studies would support this.
401 Transfusion of this blood into another individual, especially one with a compromised immune
402 system, could pose a risk of infection to the recipient. These infections might manifest not only
403 in the genital sites normally associated with the virus but also in distant vital organs, as shown in
404 this paper where the virus was found in the stomachs of four different animals. We postulate that
405 blood transmission may be one mechanism whereby papillomaviruses reach these organs and
406 subsequently contribute to cancer development.

407 To investigate the mechanism by which the virus and viral DNA are transported to local
408 tissues and induce infections therein, we tested viral binding and infection in PBMCs harvested
409 from rabbit blood. We observed the attachment of both virions and viral DNA to PBMCs, but
410 detected no viral transcripts after three days of incubation, indicating no active infection occurred
411 in these cells. These findings agree with reports in the literature that PBMCs are capable of
412 binding and transporting virus via the circulatory system (Bodaghi et al., 2005a). Further studies
413 will be needed to determine the specific blood monocytes preferred for viral attachment.

414 The link between a blood transfusion and a cancer that manifests much later in life would
415 not be easy to detect in hindsight. In view of the results presented, it would seem prudent to
416 screen blood routinely for HPV and to take steps to eliminate the pathogens when found.
417 However, many questions remain unanswered. Among them: 1) Is there a threshold viral load
418 beyond which blood-borne virus does not constitute a threat? 2) Are certain blood products free
419 of virus? We have shown that PBMCs bind both virus and viral DNA. Other studies have
420 demonstrated that viral DNA can be detected in serum and plasma (Cocuzza et al., 2017; Jeannot

421 et al., 2016). We have detected viral DNA in serum of the infected mice. However, we have not
422 yet investigated other blood products. 3) Is there an effective way to eliminate PV from donated
423 blood? These and other questions will be the focus of future studies. It is not necessary to answer
424 them, however, to conclude from the data generated to date that the presence of viral sequences
425 in the blood could pose a long-term risk for patients receiving transfusions of whole blood or
426 specific blood components. Therefore, we recommend the screening of all blood for the presence
427 of papillomavirus sequences until such time that it can be proven that the presence of HPV does
428 not pose a risk.

429 In summary, we have demonstrated, using two different animal models, that
430 papillomaviruses can be transmitted through the blood and become infectious in recipients.
431 Furthermore, transfusion of blood from an animal that had received virus via intravenous
432 infection to a naïve sibling resulted in papillomas in the transfusion recipient. Finally, we have
433 demonstrated in the mouse model that virus delivered via blood can produce active infections in
434 the stomach. These results are provocative and call into question the serious implications of HPV
435 in the human blood supply. Our findings suggest that the human blood supply could be a
436 potential source of HPV infection. They further hint at a way that papillomaviruses might come
437 to infect internal organs and set the stage for the development of cancers.

438

439 **MATERIALS AND METHODS**

440 *Animals and viral infections*

441 All rabbit and mouse work was approved by the Institutional Animal Care and Use
442 Committee of Pennsylvania State University's College of Medicine (COM) and all procedures
443 were performed in accordance with the required guidelines and regulations. Outbred New

444 Zealand White (NZW) rabbits were purchased from Robinson and maintained in our animal
445 facilities. HLA-A2.1 transgenic rabbits based on outbred NZW background were developed and
446 maintained in our animal facilities (Hu et al., 2007c). The rabbits were housed individually. Male
447 and female Hsd: NU outbred nude mice (Foxn1^{nu/nu}) (6-8 weeks old) were obtained from
448 ENVIGO. All mice were housed (2-3 mice/cage) in sterile cages within sterile filter hoods and
449 were fed sterilized food and water in the COM BL2 animal core facility.

450

451 ***Viral stock***

452 Infectious virus was isolated from cottontail rabbit tumors or tumors on the tails of mice
453 from our previous study (Cladel et al., 2016; Hu et al., 2007a). In brief, papillomas from the
454 cottontail rabbits and tumors scraped from the tails of the mice were homogenized in phosphate-
455 buffered saline (1×PBS) using a Polytron homogenizer (Brinkman PT10-35) at highest speed for
456 three minutes while chilling in an ice bath. The homogenate was spun at 10,000 rpm and the
457 supernatant was decanted into Eppendorf tubes for storage at -20°C. For these experiments, the
458 MmuPV1 was diluted 1:5 in 200 µl of 1×PBS and was passed through a 0.2 µm cellulose acetate
459 sterile syringe filter. Viral DNA extracted from 5 µl of this virus stock was quantitated using
460 qPCR as described (Hu et al., 2015).

461

462 ***Titration of infectious CRPV virus and viral DNA***

463 Viral skin infections can be initiated with either infectious virions isolated from the
464 infected tissues of wild cottontail rabbits (Cladel et al., 2008) or viral DNA cloned into a plasmid
465 vector (Kreider et al., 1995; Xiao and Brandsma, 1996). Our earlier work demonstrated the
466 benefit obtained by wounding prior to infection and supported the theory that wounding is an

467 important prerequisite for papillomavirus infection (Cladel et al., 2008). To identify the optimal
468 concentration for both virions and viral DNA infections in the New Zealand White (NZW)
469 domestic rabbits for the current study, titration studies were conducted using the pre-wounding
470 skin infection method developed in our laboratory. Titration results demonstrated that more than
471 2.75×10^6 virion DNA equivalents (Supplementary Table 1) and 1.3×10^{10} copies for cloned
472 infectious CRPV DNA (Supplementary Table 2) are required to guarantee 100% tumor
473 appearance at locally infected sites. However, as few as 2.75×10^3 virion DNA equivalents or
474 1.3×10^9 copies of the cloned infectious CRPV DNA were sufficient to generate clinical
475 infections and papillomas at a subset of pre-wounded sites. No visible tumors could be detected
476 if doses of virions or infectious viral DNA below these thresholds were delivered locally in
477 prewounded sites. For the current study, 500 μ l of infectious virus stock (2.75×10^{10} virion DNA
478 equivalents) and 500 μ g of the cloned infectious CRPV DNA (estimated to be 4.6×10^{11} copies
479 / μ l blood) were used for IV infection to maximize the chances for disease development in this
480 model.

481

482 ***Routes of infection and sample collection***

483 CRPV infectious virions used in the current study were from a viral stock previously
484 reported (Hu et al., 2014). CRPV DNA was cloned into a pUC19 vector as described in our
485 previous publications (Hu et al., 2009). Animal back skin sites were pre-wounded three days
486 before infection using our established pre-wounding techniques (Cladel et al., 2008a). For local
487 infections, the rabbits were challenged with either virions or viral DNA at the pre-wounded sites
488 (Hu et al., 2007b). To investigate whether intravenous (IV) infection with virions (500 μ l of the
489 viral stock = 2.75×10^{10} viral DNA equivalents) and viral DNA (500 μ g of plasmid = 4.6×10^{11}

490 copies / μ l blood) could induce tumors at distant susceptible back sites, six to eight back skin sites
491 of different groups of rabbits were shaved and pre-wounded with a scalpel blade as previously
492 described (Cladel et al., 2008) three days prior to IV infection. Virus or viral DNA was delivered
493 via the marginal ear vein and then back skin sites were gently re-wounded with a 28G needle
494 (Cladel et al., 2008). The infected animals were monitored for tumor growth weekly and tumors
495 were measured and documented photographically. Rabbits were euthanized up to 12 weeks after
496 initial viral infection, and tissues were collected for cellular, molecular, and histological
497 analyses. Blood samples were collected from the intravenously infected rabbits at different time
498 points. DNAs extracted from the whole blood using a blood DNA extraction kit from QIAGEN
499 were used for viral DNA detection. Serum samples were harvested for the detection of anti-viral
500 antibodies (Hu et al., 2007a). Peripheral blood mononuclear cells (PBMCs) were isolated from
501 the blood samples and tested for viral sequences (Hu et al., 2010b). PBMCs were also harvested
502 from naïve rabbits for in vitro binding and infection studies. To infect PBMCs, 5 μ l of CRPV
503 virions or 1 μ g of viral DNA were incubated with 1×10^6 rabbit PBMCs in vitro for 3-4 days at
504 37°C in RPMI1640 complemented with 10% FBS (Hyclone). The RNA was extracted and
505 examined for the presence of viral transcripts as previously described (Hu et al., 2007a). To
506 investigate whether transfusions of blood from an animal that had received virus (500 μ l of the
507 viral stock = 2.75×10^{10} viral DNA equivalents) by IV injection could transmit infection to naive
508 siblings, 10 ml of blood was drawn from the injected animal heart 25 minutes post IV infection
509 and transfused via IV injection into naive animals with pre-wounded back sites. Recipients were
510 monitored for tumor growth and measurements were recorded. Rabbits were euthanized up to 12
511 weeks after viral infection, and tissues were collected for cellular, molecular, and histological
512 analyses.

513 In addition to the CRPV/rabbit model, we used the more recently established
514 MmuPV1/mouse model for a number of our studies (Hu et al., 2017). Female mice were
515 subcutaneously inoculated with 3 mg Depo-Provera (Pfizer) in 100 μ l PBS three days before the
516 viral infection as previously described (Cladel et al., 2015). Mice were sedated intraperitoneally
517 with 0.1ml/10 g body weight with ketamine/xylazine mixture (100 mg/10 mg in 10 ml ddH₂O).
518 The lower genital (vaginal) and anal tracts were wounded with Doctors' Brush Picks coated with
519 Conceptrol (Ortho Options, over the counter) as previously described (Hu et al., 2015). Tongues
520 were withdrawn using a sterile forceps and microneedles were used to wound the ventral surface
521 of the tongues (Cladel et al., 2016; Hu et al., 2015). Twenty-four hours after wounding, eight
522 female and six male Hsd: Nu athymic mice were again anesthetized and challenged with
523 infectious MmuPV1 virions (1×10^8 viral DNA equivalents) via the tail vein. The injection sites
524 were topically treated with neutralizing antibody (MPV.A4) immediately post injection to
525 neutralize any virions remaining at the injection site. Monitoring was conducted weekly for
526 infection at muzzle and tail and progress was documented photographically at these two
527 cutaneous sites for each animal (Cladel et al., 2017a; Cladel et al., 2017b). Viral infection at
528 three mucosal sites (vagina or penis, anus and tongue) was monitored for viral DNA using swabs
529 or by lavage as described previously (Hu et al., 2015). At the termination of the experiment,
530 selected organ tissues (kidney, lung, liver, spleen, stomach, and bladder) were harvested to
531 determine whether viral infections could be detected in other unanticipated sites. The tissues
532 were analyzed histologically for the presence of viral DNA and/or capsid protein production.

533 To investigate whether blood from actively infected mice could transmit the infection to
534 naïve animals, blood was withdrawn from one infected male and one infected female mouse and
535 transfused by tail vein injection to three naïve male and female mice respectively. The injection

536 sites were treated topically with neutralizing antibody (MPV.A4) immediately post injection to
537 neutralize any virions remaining at the site. The mice were maintained for up to six months post
538 infection and tissues were collected for cellular, molecular, and histological analyses. Vaginal
539 and anal lavages were conducted using 25 μ l of sterile 0.9% NaCl introduced into the vaginal
540 and anal canals with a disposable filter tip. The rinse was gently pipetted in and out of the canals
541 and stored at -20°C before being processed for DNA extraction (Hu et al., 2015). For oral lavage,
542 a swab (Puritan Purflock Ultra, Puritan Diagnostics LLC) soaked in 25 μ l of sterile 0.9% NaCl
543 was used (Cladel et al., 2017b). For DNA extraction, the DNeasy kit (QIAGEN) was used
544 according to the instructions of the manufacturer. All DNA samples were eluted into 50 μ l EB
545 buffer (Hu et al., 2015).

546

547 ***RNA isolation from rabbit tumors for quantitative PCR assays***

548 Tumor tissues of NZW rabbits with CRPV infections induced by two different routes, a)
549 local skin infection and b) ear IV injection, were harvested for QPCR analysis of host genes
550 (Table 1). The tissues were homogenized in TriPure reagent (Roche). Total RNA was extracted
551 according to the TriPure extraction protocol and treated with the TURBO DNA-free™ Kit
552 (Ambion) to eliminate all traces of viral DNA. The integrity of RNA were evaluated by an
553 Agilent DNA bioanalyzer and quantified by NanoDrop. Reverse Transcription (RT) was
554 performed with the SuperScript II kit (Thermo Fisher Scientific). 1 μ g of total RNA from each
555 tissue was used per reverse transcription reaction to synthesize single-stranded cDNA. cDNA
556 samples were further analyzed using the TaqMan Universal PCR Master Mix (Thermo Fisher)
557 by a StepOne Plus Real-Time PCR System (Applied Biosystems). To avoid interplate variability,
558 differentially expressed gene expression analyses were performed using a single 96-well plate in
559 triplicate. GAPDH was used as an internal control and analyzed in the same plate for each

560 sample. Each threshold cycle (Ct) value of real-time quantitative PCR data from three repeats
561 was individually normalized to GAPDH and analyzed by the $2^{-\Delta\Delta Ct}$ method (Xue et al., 2017).
562 All primers and Taqman probes used were listed in Table 3.

563

564 *RNA-seq Analysis*

565 Total RNA isolated using TriPure Reagent (Roche) and the RNeasy Mini kit with on-
566 column DNase-treatment (Qiagen) was used for RNA-seq analysis. The sequencing libraries
567 were constructed from Ribo-minus RNA using TruSeq Stranded Total RNA kit (Illumina RS-
568 122-2201). The obtained libraries were then pooled and sequenced using Illumina TruSeq v4
569 chemistry, 125-bp paired-end, with 100 million reads depth. The HiSeq RT Analysis software
570 (RTA v1.18.64) was used for base calling. The Illumina bclfastq v2.17 software was used to
571 demultiplex and convert binary base calls and qualities to FASTQ format. The obtained reads
572 were mapped first to the oryCun2.0 (*Oryctolagus cuniculus*) reference genome
573 (https://www.ncbi.nlm.nih.gov/assembly/GCF_000003625.2/) to which had been added a contig
574 containing the cottontail rabbit papillomavirus (CRPV) Hershey strain reference genome
575 (GenBank Acc. No. JF303889.1) permuted at nt 7421. The viral read coverage along the CRPV
576 reference genome was then visualized using the IGV software
577 (<http://software.broadinstitute.org/software/igv/>). To determine the changes in host gene
578 expression upon viral infection, the reads were remapped to the oryCun2.0 reference genome
579 without the CRPV contig. RNA-seq NGS-datasets were processed using the CCBP Pipeliner
580 utility (<https://github.com/CCBR/Pipeliner>). Briefly, reads were trimmed of low-quality bases
581 and adapter sequences were removed using Trimmomatic v0.33 (Bolger et al., 2014). Mapping
582 of reads to the oryCun2.0+CRPV reference genome was performed using STAR v2.5.2b in 2-

583 pass mode (Dobin et al., 2013). Then, RSEM v1.3.0 was used to quantify gene-level expression,
584 with counts normalized to library size as counts-per-million (Dobin et al., 2013). Finally, limma-
585 voom v3.34.5 was used for quantile normalization and differential expression (Li and Dewey,
586 2011). The data discussed in this publication have been deposited in NCBI's Gene Expression
587 Omnibus (Phipson et al., 2016) and are accessible through GEO Series accession number
588 GSE124211. Genes were considered to be attributed to CRPV infection if they were significantly
589 (adjusted $p \leq 0.05$) differentially expressed relative to control with absolute fold change relative
590 to control ≥ 2.0 . Genes with "unknown" gene symbols in the oryCun2.0 gene annotation dataset
591 were quantified but excluded from further analysis in this manuscript. Expression data were
592 visualized as heat maps using ClustVis (Metsalu and Vilo, 2015).

593

594 ***Viral DNA copy number analysis***

595 Linearized MmuPV1 genome DNA was used for standard curve determination by Probe
596 qPCR analysis (Brilliant III Ultra-Fast QPCR Master Mix, Agilent). The primer pairs (5'-
597 GGTTGCGTCGGAGAACATATAA-3' and 5'-CTAAAGCTAACCTGCCACATATC-3') and the
598 probe 5'-FAM-TGCCCTTTCA/ZEN/GTGGGTTGAGGACAG-3'-IBFQ-3') that amplify the
599 viral E2 region were used. The qPCR reactions were run in AriaMx program (Agilent). Each
600 reaction consisted of 500 nM specific primer pairs and 250 nM double-labeled probes. PCR
601 conditions were: initial denaturation at 95 °C for 10 min, then 40 cycles at 95°C for 10 min,
602 followed by 40 cycles consisting of denaturation at 95°C for 15 s and hybridization of primers and
603 the probe as well as DNA synthesis at 60 °C for 1 min. All samples were tested in at least
604 duplicates. Viral titers were calculated according to the standard curve. Viral copy numbers in 2 µl
605 of a 50 µl DNA lavage extract were converted into equivalent DNA load using the formula 1 ng

606 viral DNA = 1.2×10^8 copy numbers (<http://cels.uri.edu/gsc/cndna.html>). In some cases we also
607 calculated the difference in cycle time (Ct) between the 18S rRNA gene and viral DNA (Δ Ct) (Hu
608 et al., 2015). Fold change ($2^{-\Delta\Delta$ Ct) demonstrates the relative viral DNA load in each sample as
609 previously described (Cladel et al., 2017a).

610

611 ***Antibody detection by ELISA***

612 Rabbit and mouse sera were collected at the termination of the experiment. CRPV or
613 MmuPV1 virus-like particles (VLPs) were used as the antigen for ELISA. Anti-CRPV
614 monoclonal antibody (CRPV.1A) or anti-MmuPV1 monoclonal antibody (MPV.A4) was used as
615 positive control and the sera of non-infected animals as negative control for the corresponding
616 antigens. The ELISA was conducted as previously reported (Hu et al., 2014).

617

618 ***In vitro neutralization assay***

619 A rabbit cell line (RA2LT) generated in house was used for in vitro neutralization for
620 serum collected from the CRPV infected rabbits (Hu et al., 2010). A mouse keratinocyte cell line
621 (K38, a generous gift from Dr. Julia Reichelt, University of Newcastle, UK) was seeded at 1.5
622 $\times 10^5$ cells per well in DMEM/Ham's F-12, with 4.5 g/l D-Glucose, 50 μ M CaCl₂, with L-
623 Glutamine and Na-Pyruvate (Cedarlane), in 10% FBS with calcium depleted at 32°C. One μ l of
624 viral extract from tail papillomas was incubated with various dilutions of mouse sera (1:50-1:100
625 dilution) in media for 1 hr at 37°C and added onto K38 cells incubated in 12-well plates at 32°C
626 for 72 hours. The cells were harvested with TRIzol reagent (Thermo Fisher).

627

628 ***CRPV E1^{E4} detection by RT-qPCR***

629 Total RNA was extracted from the infected cells, and infectivity was assessed by
630 measuring viral E1^{E4} transcripts with RT-qPCR (E1^{E4}-forward, 5'-CATTCGAGTC
631 ACTGCTTCTGC-3'; E1^{E4}-reverse, 5'-GATGCAGGTTTGTCGTTCTCC-3'; E1^{E4}-probe,
632 5'-6-carboxyfluorescein (FAM)-TGGAAAACGATAAAGCTCCTCCTCAGCC-6-
633 carboxytetramethylrhodamine (TAMRA)-3' as previously described with a few modifications as
634 follows: The Brilliant III RT-qPCR Master Mix (Agilent) was used for the RT-qPCR reactions.
635 The following cycling conditions were applied: 50°C for 30 minutes (the reverse transcription),
636 95°C for 10 minutes, and 40 cycles of 94°C for 15 seconds and 60°C for 1 minute. At the end of
637 each amplification cycle, three fluorescence readings were detected. Analysis of the
638 amplification efficiencies was performed using the REST software (Cladel et al., 2017a).

639
640 ***Western blot analysis***

641
642 Total protein from matching samples used in the RNA-seq study was isolated by
643 homogenization in 1 × RIPA (Boston BioProducts) buffer supplemented by 1 × complete
644 protease inhibitors (Roche). The isolated total protein was analyzed by Western blot for the
645 expression of endogenous protein using specific antibody against APOBEC2 (Sigma-Aldrich,
646 cat. no. SAB2500083), S100A9 (Abnova, cat. no. PAB11470) and β-tubulin (Sigma-Aldrich, cat.
647 no. T5201).

648

649 ***Immunohistochemistry and in situ hybridization analyses of infected tissues***

650 After termination of the experiment, the animals were euthanized, and tissues of interest
651 were fixed in 10% buffered formalin and processed to formalin-fixed paraffin-embedded (FFPE)
652 sections as previously described (Cladel et al., 2015). Hematoxylin and eosin (H&E) analysis, in
653 situ hybridization (ISH) and immunohistochemistry (IHC) were conducted as described in

654 previous studies (Cladel et al., 2015; Hu et al., 2015). For IHC, an in-house anti-MmuPV1 L1
655 monoclonal antibody (MPV.B9) was used on FFPE sections. For ISH, a biotin labeled 3913bp
656 EcoRV/ BamHI sub genomic fragment of MmuPV1 was used as an in situ hybridization probe
657 for the detection of MmuPV1 DNA in tissues (Cladel et al., 2015). Counterstaining for ISH was
658 Nuclear Fast Red (American MasterTech, Inc.) and for IHC was hematoxylin (Thomas
659 Scientific).

660

661 **ACKNOWLEDGEMENT**

662 **Funding information:** Research reported in this publication was supported by the NCI grant
663 CA47622 to N.C., NIAID grant R21AI121822 to N.C. and J.H. and the Jake Gittlen Memorial
664 Golf Tournament. This study was also supported by Intramural Research Program of NCI/NIH
665 (1ZIASC010357 to Z.M.Z) and NCI/NIH contract (HHSN261200800001E). The content of this
666 publication does not necessarily reflect the views or policies of the Department of Health and
667 Human Services, nor does mention of trade names, commercial products, or organizations imply
668 endorsement by the U.S. Government. This research was supported (in part) by the National
669 Institutes of Health.

670

671 **Conflicts of interest**

672 The authors declare that there are no conflicts of interest.

673

674 **Author Contributions**

675 Conceptualization: ZZ, JH

676 Data curation: NMC, PJ, JL, XP, TKC, TJM, MC, KKB, SAB, VM, JH

677 Formal analysis: NMC, PJ, TKC, KKB, TJM, MC, VM, JH
678 Funding acquisition: NDC, ZZ, JH
679 Investigation: NMC, JL, LRB, KKB, XP, TKC, DAS, SAB, RM, PJ, VM, RV, ZZ, NDC, JH
680 Methodology: NMC, LRB, KKB, PJ, JL, VM, SAB, TJM, MC, DAS, JH
681 Project administration: NMC, NDC, ZZ, JH
682 Resources: NDC, ZZ, JH
683 Supervision: JH, ZZ, NDC
684 Validation: NMC, PJ, JL, DAS, TKC, LRB, TJM, MC, KKB, SAB, JH
685 Visualization: NMC, JL, LRB, TJM, KKB, TKC, DAS, JH
686 Writing – original draft: NMC, JH, ZZ
687 Writing – review & editing: NMC, JL, XP, TKC, VM, TJM, ZZ, NDC, JH

688
689
690
691
692
693
694
695
696
697
698
699
700
701
702
703
704
705
706
707
708
709
710
711

712 **Table 1. Primers and probes for RT-qPCR of rabbit gene transcripts**
 713

Gene names	Primers/probes	Sequence (From 5' - to 3' -)
GAPDH	Forward primer	GACCACTTTGTGAAGCTCATTTC
	Backward primer	GTGGTTTGAGGGCTCTTACTC
	Taqman probe	ATTTGGCTACAGCAACAGGGTGGT
IL36G	Forward primer	GTTGGGAAGCTCTCCGATTT
	Backward primer	CGGATACTTGCACGGCATAA
	Taqman probe	TGACAGTTCCAAGGAGTAGCAACGC
SLN	Forward primer	CGTGTGTCCTTGACCTTCTT
	Backward primer	GTGGATCGCTCCATTCTCAG
	Taqman probe	AAGCCTGCCACAAGTTCTCACTGA
MYH8	Forward primer	CTTGGACATTGCAGGCTTTG
	Backward primer	GTTTCTCGTTGGTGAAGTTGATG
	Taqman probe	TGATTTCAACAGCCTGGAGCAGCT
FABP9	Forward primer	CAGAACAGAGAGTCCTTTCAGG
	Backward primer	GAGCCACTGTCCAATGTTACT
	Taqman probe	ACAGCAGACAACCGGAAAGTGAAGA
PGAM2	Forward primer	CCCTTCTGGAACGAGGAGAT
	Backward primer	GGCAGATTCAGCTCCATGAT
	Taqman probe	CAAACACCTGGAAGGGATGTCGGA
KRT16	Forward primer	GAGCTACGCAGGGTGTTTC
	Backward primer	GTAGCGGCCTTTGGTCTC
	Taqman probe	AGGCTGTTCTCCAGGGATGCTTTC
SDR9C7	Forward primer	GGCTACTGTGTCTCCAAGTTT
	Backward primer	CCCAGGCTCAATGATGCTAA
	Taqman probe	CCTTCTCTGACAGCATCAGGCGTG

714 Note: Taqman assays of TAC1 (Thermo Fisher 5'-FAM,3'-MGB, predesigned, premixed, Assay
 715 ID: Oc03399333_m1) and S100A9 (Thermo Fisher 5'-FAM,3'-MGB, predesigned, premixed,
 716 Assay ID: Oc03395775_m1) were ordered from Thermo Fisher.
 717

718

719

720

721

722

723

724

725 **FIGURE LEDENDS**

726 **Figure 1. Tumor growth patterns resulting from IV infection with CRPV virions via**
727 **marginal ear vein injection. (A-C)** Two NZW rabbits (NZW#1-2) and one HLA-A2.1
728 transgenic rabbit (A2) infected by IV injection of virions equivalent to 2.75×10^{10} copies of viral
729 DNA displayed tumors that mimic those by local skin infections in our previous studies (Hu et
730 al., 2007b). **(D)** Tumor growth on one (NZW#1) of the three animals at week 11 post infection
731 was shown. **(E)** one (NZW#3) of four additional rabbits (NZW#3-6) infected by IV injection of
732 virions equivalent to 5.5×10^9 viral DNA equivalents developed tumors at six weeks post
733 infection. Both tumors (D and E) exhibited similar appearance of tumors from local skin infected
734 with high to low dilutions of virus at week six post infection **(F)**. **(G, I)** The tumors induced via
735 marginal ear vein (IV) infection have similar morphology and histology (H&E, 20 \times) to those **(K)**
736 initiated by local infections (H&E, 20 \times). **(H, J and L)** On the surface of the mass there was a
737 subcorneal cleft filled with erythrocytes and fibrin with frequent heterophils (hemorrhagic
738 vesicle), with scattered smaller acute stromal and intra-epithelial hemorrhages. No interface
739 inflammation was detected in these tumors. Viral DNA was detected by *in situ* hybridization
740 (ISH in tumors induced by both intravenous and local skin infections (20 \times , arrows).

741
742 **Figure 2. Neutralizing antibodies were induced in the intravenously infected rabbits.**
743 Positive control was anti-rabbit L1 (CRPV.1A) (Christensen and Kreider, 1991) and the negative
744 control was serum of a non-infected rabbit for both ELISA and in vitro neutralization analyses.
745 All seven IV infected animals generated specific anti-CRPV antibodies. **(A)** The antibody titer in
746 ELISA assay was not correlated with the tumor size. **(B)** These anti-CRPV antibodies were
747 neutralizing by the in vitro neutralizing assay.

748

749 **Figure 3. Viral RNA transcripts in four tumor lesions of four individual rabbits IV infected**

750 **by CRPV virions through marginal ear vein injection.** Total RNA isolated from each tumor

751 and depleted of ribosomal RNA was analyzed by RNA-seq. By mapping the RNA-seq raw reads

752 to the newly arranged linear CRPV genome starting from nt 7421 and ending at nt 7420 using

753 RNA sequence aligner TopHat, we obtained 18318, 24014, 62100, and 128869 viral reads for the

754 respective tumor tissues; this accounts for 0.0290%, 0.0442%, 0.0911%, and 0.1960% of total

755 RNA reads obtained from each sample, respectively. By uploading these uniquely mapped viral

756 RNA reads to the Integrative Genomics Viewer (IGV) program to visualize reads coverage

757 profile along with the CRPV genome, we found three major coverage peaks in the E6, E7 and

758 E1^E4 regions among all tumor tissues.

759

760 **Figure 4. Dysregulation of the host transcriptome by CRPV infection. (A)** Principle

761 component analysis of the ten RNA-seq samples. **(B-C)** Volcano plots of 17742 annotated genes

762 assayed in each contrast of our analysis. The x-axis is the log₂ fold change in expression (note

763 the x-axes of each panel are not to the same scale). The y-axis is *p*-value adjusted for multiple

764 comparisons. Red dots indicate the genes with both significant differential expression and large

765 absolute fold change relative to control; black dots indicate those genes that do not met these

766 criteria. Vertical dashed lines represent fold change thresholds (absolute fold change ≥ 2.0) and

767 horizontal dashed lines represent the significance threshold (adjusted $p \leq 0.05$). **(D)** Venn

768 diagram of all 5224 genes with differential expression (adjusted $p \leq 0.05$ and absolute fold

769 change ≥ 2.0) in the wart tissues induced by local skin or IV CRPV infection over the normal

770 control skin tissues. Numbers with arrows indicate the number of genes (after all filters) up- and

771 down-regulated in each experimental group relative to control group. **(E)** Heat map showing the
772 top 100 up-regulated and top 100 down-regulated genes with significantly differential expression
773 common both in the tumors induced by both local skin and IV infections, relative to control. A
774 color scale bar represents relative gene expression level within centered rows. Unit variance
775 scaling has been applied to rows. Both rows and columns are clustered using Euclidean distance
776 and complete linkage.

777

778 **Figure 5. Representative host genes with differential expression in skin tumors induced by**

779 **both routes of CRPV infections. (A)** Heat map showing the expression of 9 selected host genes

780 chosen based on their expression abundance and cellular functions. A color scale bar represents

781 relative gene expression level within centered rows. Unit variance scaling has been applied to

782 rows. Both rows and columns are clustered using Euclidean distance and complete linkage. **(B)**

783 Verification of differentially expressed rabbit genes in RNA-seq results by real-time qPCR.

784 Consistent with RNA-seq data, SLN, TAC1, MYH8, and PGAM2 were down-regulated in both

785 CRPV blood infection (Animal #9, #11, and #12) and CRPV skin infection (Animal#6, #7, and

786 #8) animals relative to those in normal control animals, whereas SDRC7, KRT16, S100A9,

787 IL36G, and FABP9 were up-regulated in both CRPV skin infection and CRPV blood infection

788 animals compared to normal controls. The Y-axis indicates relative gene expression levels

789 calculated by $2^{-\Delta\Delta C_T}$ and the X-axis indicate the different samples. NC, gene expression in the

790 normal tissue, was set to 1 after normalization to GAPDH. **(C)** Western blot analysis of

791 representative samples from normal skin and warts induced by cutaneous or intravenous (IV)

792 CRPV infection for the expression of S100A9 and Apobec2. Cellular β -tubulin served as loading

793 control.

794

795 **Figure 6. Tumor growth by IV infection with CRPV DNA via marginal ear vein. (A)** Three

796 tumors were detected at pre-wounded back skin sites on one rabbit at week nine post

797 intravenously infected with CRPV DNA via the marginal ear vein injection. **(B)** There are

798 multifocal dense leukocytic infiltrates at the dermal-epidermal junctions within the tumor mass,

799 predominantly macrophages with fewer lymphocytes and rare neutrophils in a representative

800 tumor (H&E, 20×). Epithelial polarization and differentiation are maintained from basement

801 membrane to the surface, with occasional mitoses and mild nuclear atypia. There are occasional

802 koilocytosis and scattered individual apoptotic keratinocytes within the epithelium. There is no

803 invasion present in examined tissues. This tumor has similar histology to those initiated by local

804 skin infection as shown in Fig. 1 K.

805

806 **Figure 7. Tumor growth on blood transfusion recipient. (A)** A tumor was detected at one

807 recipient rabbit's back pre-wounded skin site at week ten after receiving a blood transfusion from

808 a rabbit that had been infected via the ear vein with 1.8×10^5 viral DNA equivalents / μ l blood for

809 30 minutes. **(B)** The tumor has exophytic polypoid cutaneous warty masses similar to Fig. 4B,

810 but with minimal inflammation. There is a mixture of ortho- and parakeratotic debris on the

811 surface of the masses. **(C)** Viral DNA was detected in the tumor by in situ hybridization (ISH,

812 60×).

813

814 **Figure 8. Tumor growth at cutaneous sites (muzzle and tail) and viral DNA detection at the**

815 **four mucosal (vaginal, V; Penile, P; Anal, A and Oral, O) sites after MmuPV1 IV infection**

816 **via the tail vein.** Infections were introduced via the tail vein with 1×10^8 viral DNA equivalent

817 virions in eight Hsd: Nu female and six male mice that had been pre-wounded according to our

818 standard protocol. The injection sites were treated topically with an excess of neutralizing
819 antibody (MPV.A4) immediately post injection to neutralize any virions remaining at the site
820 (Cladel et al., 2017b). **(A, C)** The animals were monitored for tumor growth at pre-wounded
821 cutaneous sites and **(B, D)** for viral DNA detection by Q-PCR at mucosal sites. **(E)** Tongue, **(F)**
822 Vaginal, **(G)** Anal, (all 20×), were positive for viral DNA by in situ hybridization (ISH).
823 Interestingly, dysplasia was found in the penile tissue (H&E, H, 10×, arrow) that was positive for
824 viral DNA by ISH **(I, 10×, K, 20×)** and viral capsid protein by immunohistochemistry **(J, 20×)**.

825

826 **Figure 9. Three (two females and one male) of eleven tested mice were positive for virus**
827 **infection in the stomach tissues.** Representative stomach tissues were examined for histology.

828 **(A)** Within the glandular stomach there is a focally extensive plaque lesion of mild to moderate
829 hyperplasia with atypia. There is abundant hyperkeratosis (likely parakeratotic), with what
830 appear to be crypt formation. There are occasional positive nuclei within the stratum spinosum
831 and granulosum, with abundant positive staining of the cornified layers. There is multifocal
832 cytoplasmic hybridization with parietal cells in the glandular stomach. **(D)** A small isolated
833 (possibly pedunculated) focus of mild hyperplasia with cytologic and nuclear atypia (low grade)
834 in the non-glandular stomach with scattered individual nuclear positive cells. These tissues were
835 positive for viral DNA by both *in situ* hybridization (ISH, **B, E, 20×**, in blue) and viral capsid
836 protein by immunohistochemistry (IHC, **C, F, 20×**, in red).

837

838 **Figure 10. Blood of MmuPV1 infected mice with skin tumors was infectious at seven**
839 **months post initial IV injection.** Each naïve littermate transfused by IV injection of 0.2 mL of
840 blood from two infected mice sacrificed seven months after initial IV MmuPV1 infection was

841 examined weekly for tumor growth at the pre-wounded skin area. (**A, B**) Representative tumor
842 growth (arrows) at the muzzle and the tail of naïve Hsd: Nu female (**A**) and male (**B**) mice at
843 week sixteen post blood transfusion. Viral DNA was detected at the vaginal (**V**), Anal (**A**) and
844 Oral (**O**) sites in three females (**C**, F1-F3) and the Penile (**P**), Anal (**A**) and Oral (**O**) sites in three
845 male (**D**, M1-M3) mice by qPCR. Mucosal sites of these mice (Vagina, Anus, Tongue, and
846 penile) were positive for viral DNA by in situ hybridization (**E**, arrows, 20×, in blue). One of the
847 females was positive for viral DNA (ISH arrows, 60×, in blue) and viral capsid protein L1 (IHC,
848 arrows, 60×, in red) in the stomach tissues (**F**).

849

850

851

852

853

854

855

856

857

858

859

860

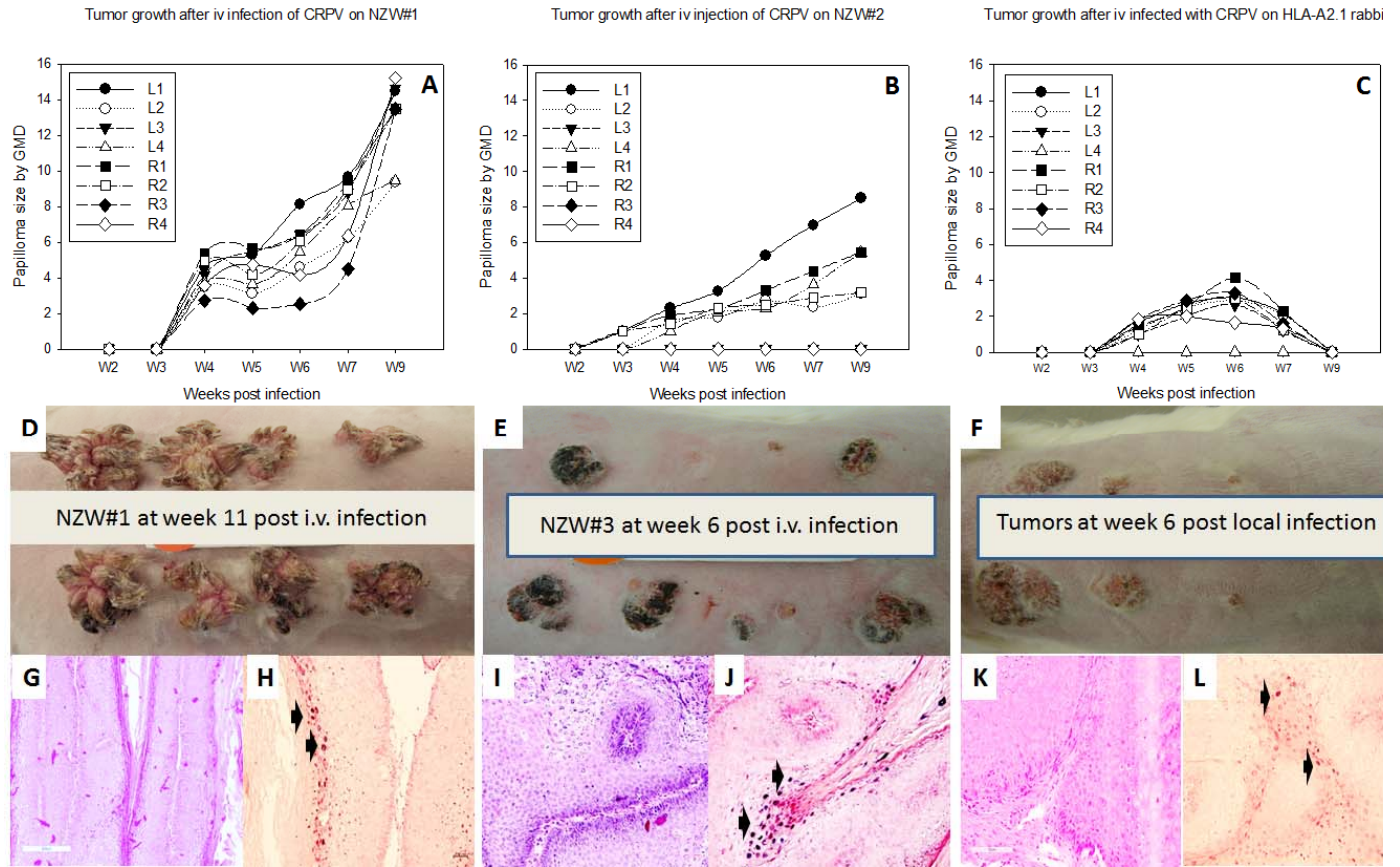
861

862

863

864 **Figure 1.**

865



866

867

868

869

870

871

872

873

874

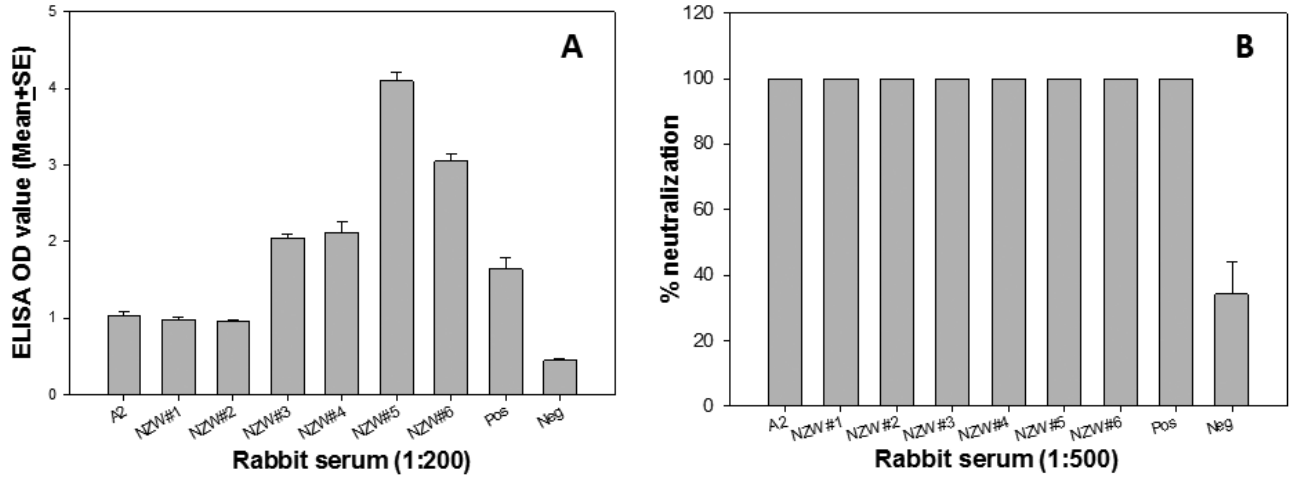
875

876

877

878 **Figure 2.**

879



880

881

882

883

884

885

886

887

888

889

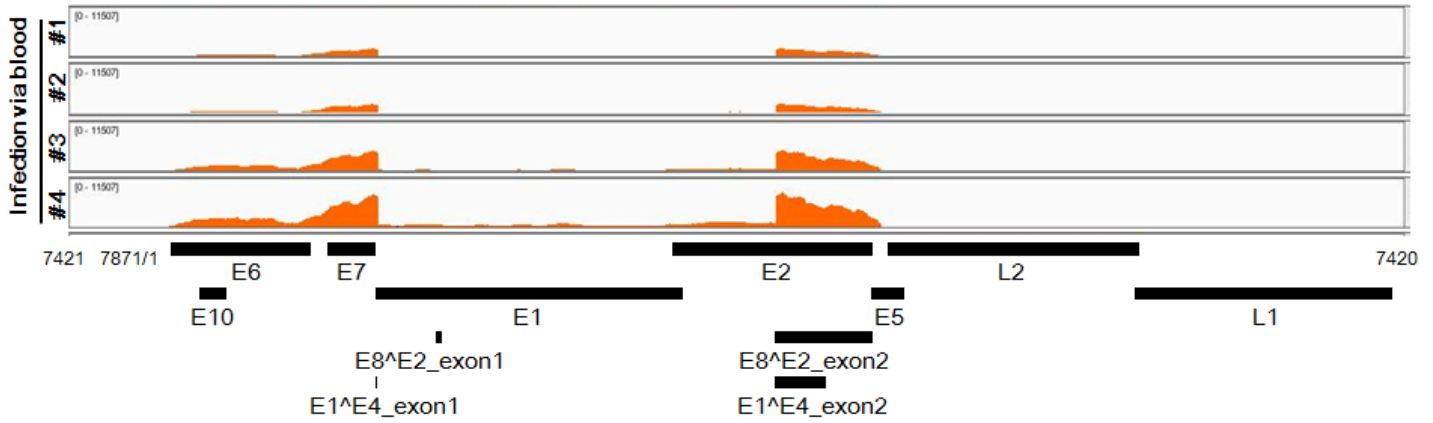
890

891

892

893

894 **Figure 3.**



895

896

897

898

899

900

901

902

903

904

905

906

907

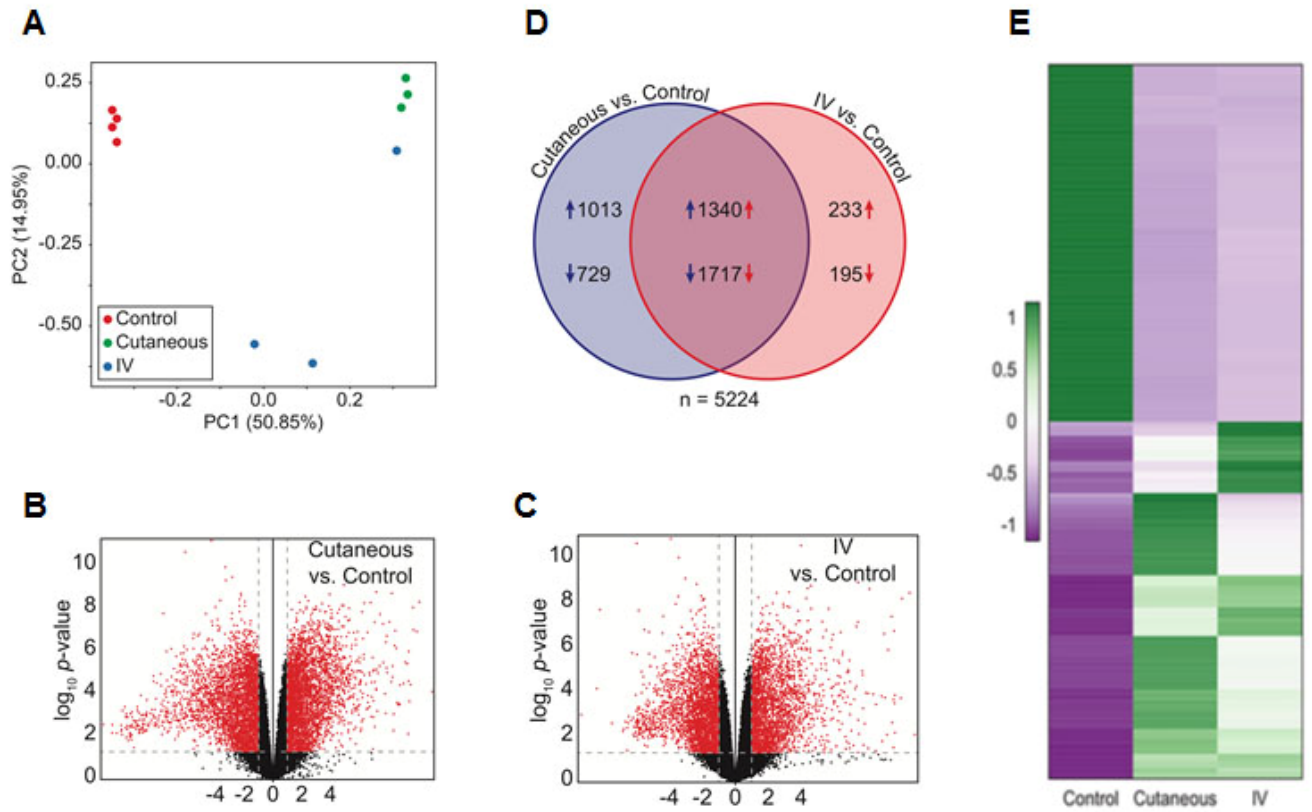
908

909

910 **Figure 4.**

911

912



913

914

915

916

917

918

919

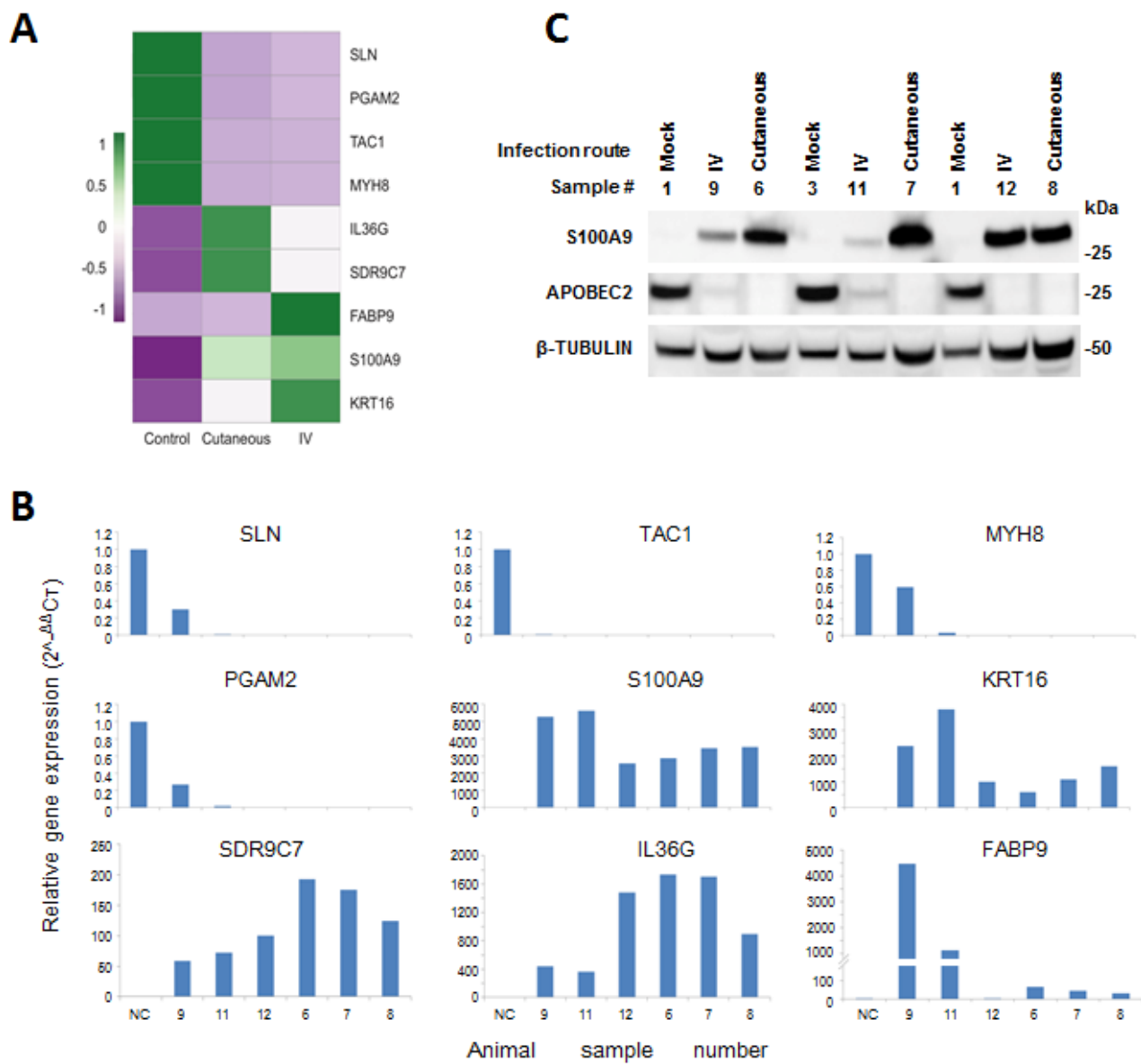
920

921

922 **Figure 5.**

923

924



925

926

927

928

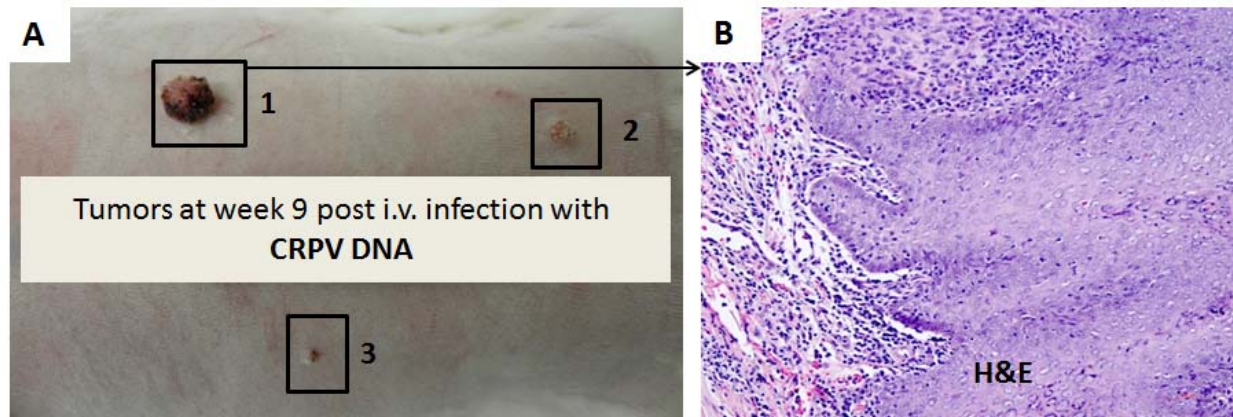
929

930 **Figure 6.**

931

932

933



934

935

936

937

938

939

940

941

942

943

944

945

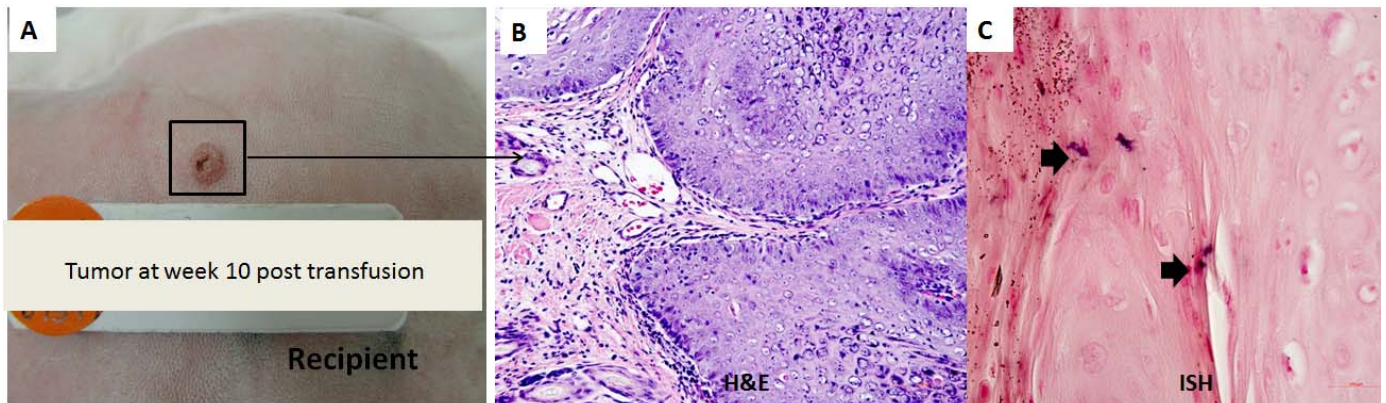
946

947

948 **Figure 7.**

949

950



951

952

953

954

955

956

957

958

959

960

961

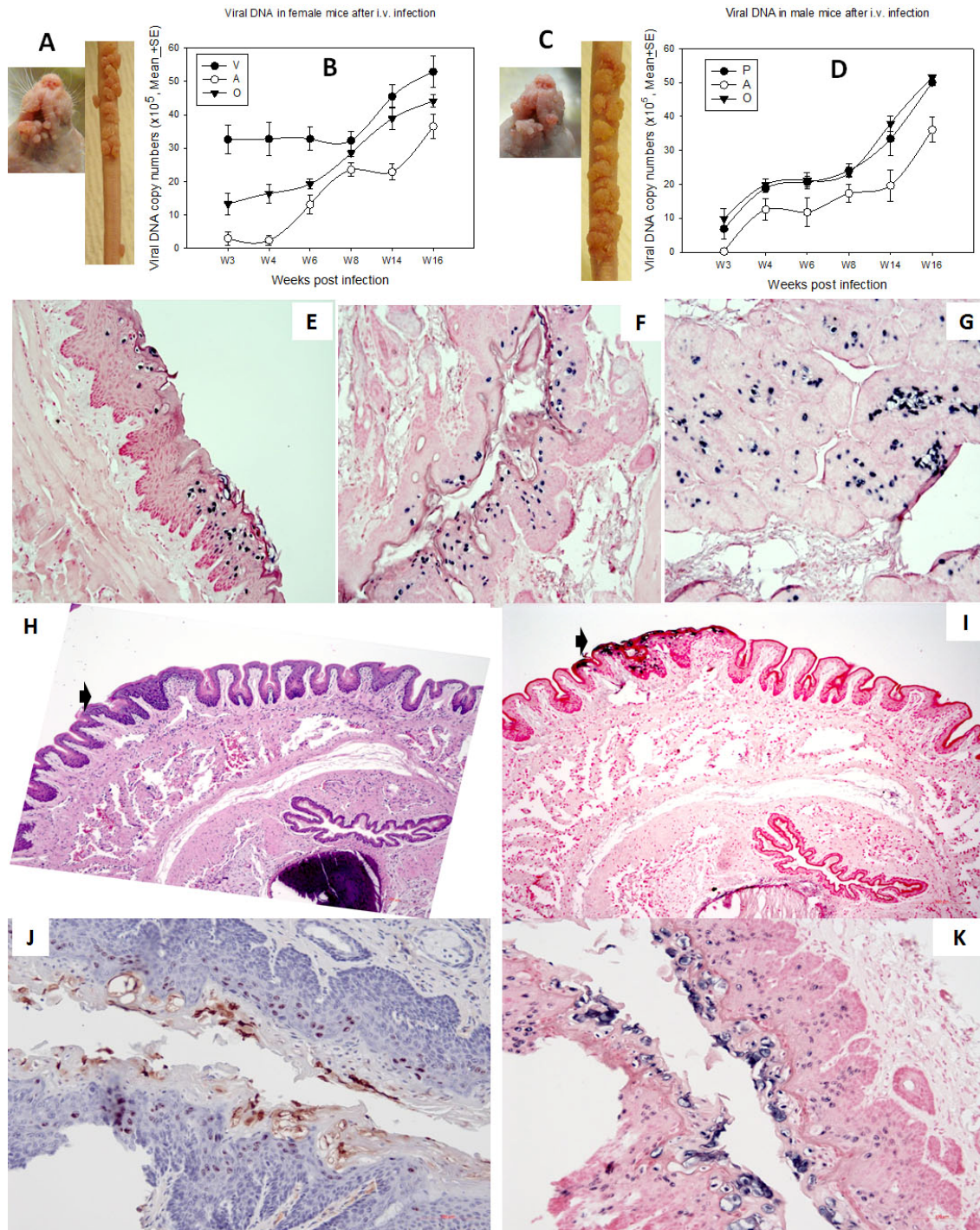
962

963

964

965 **Figure 8.**

966



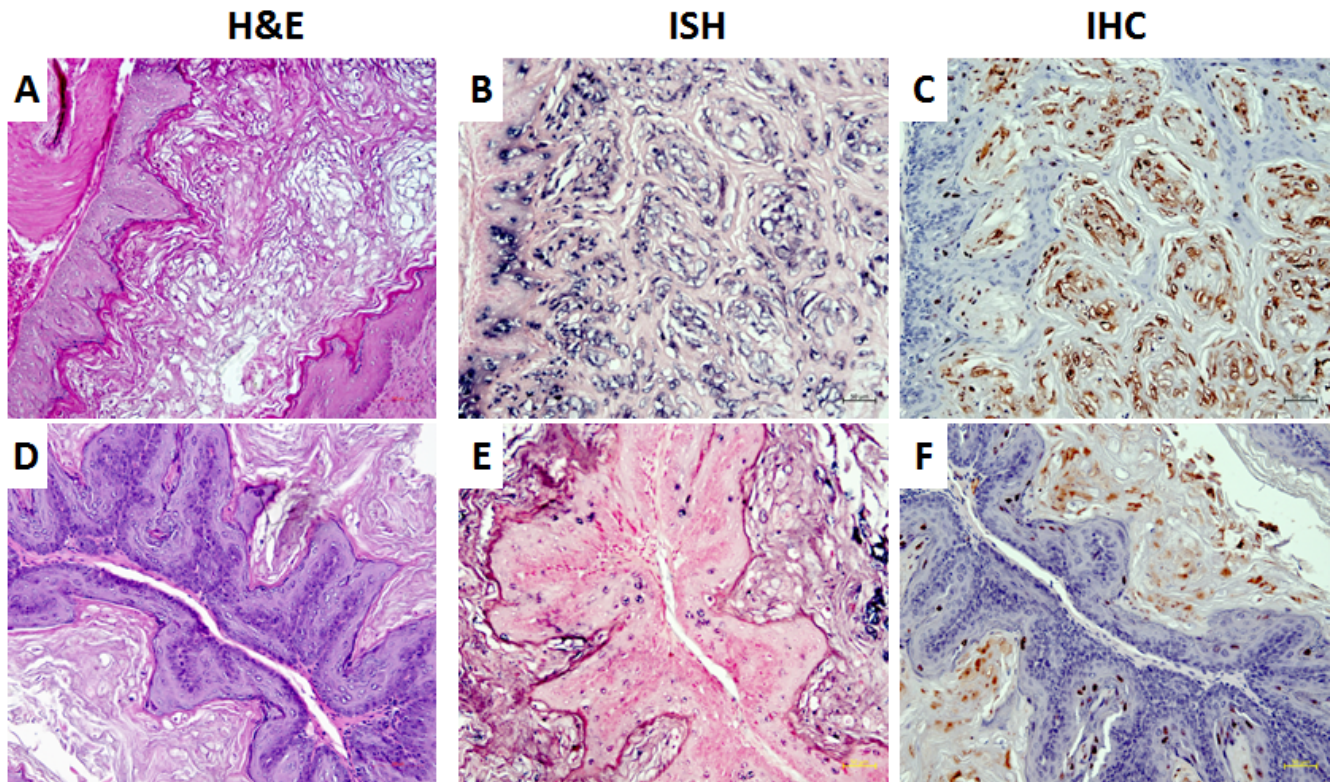
967

968

969

970

971 **Figure 9.**



972

973

974

975

976

977

978

979

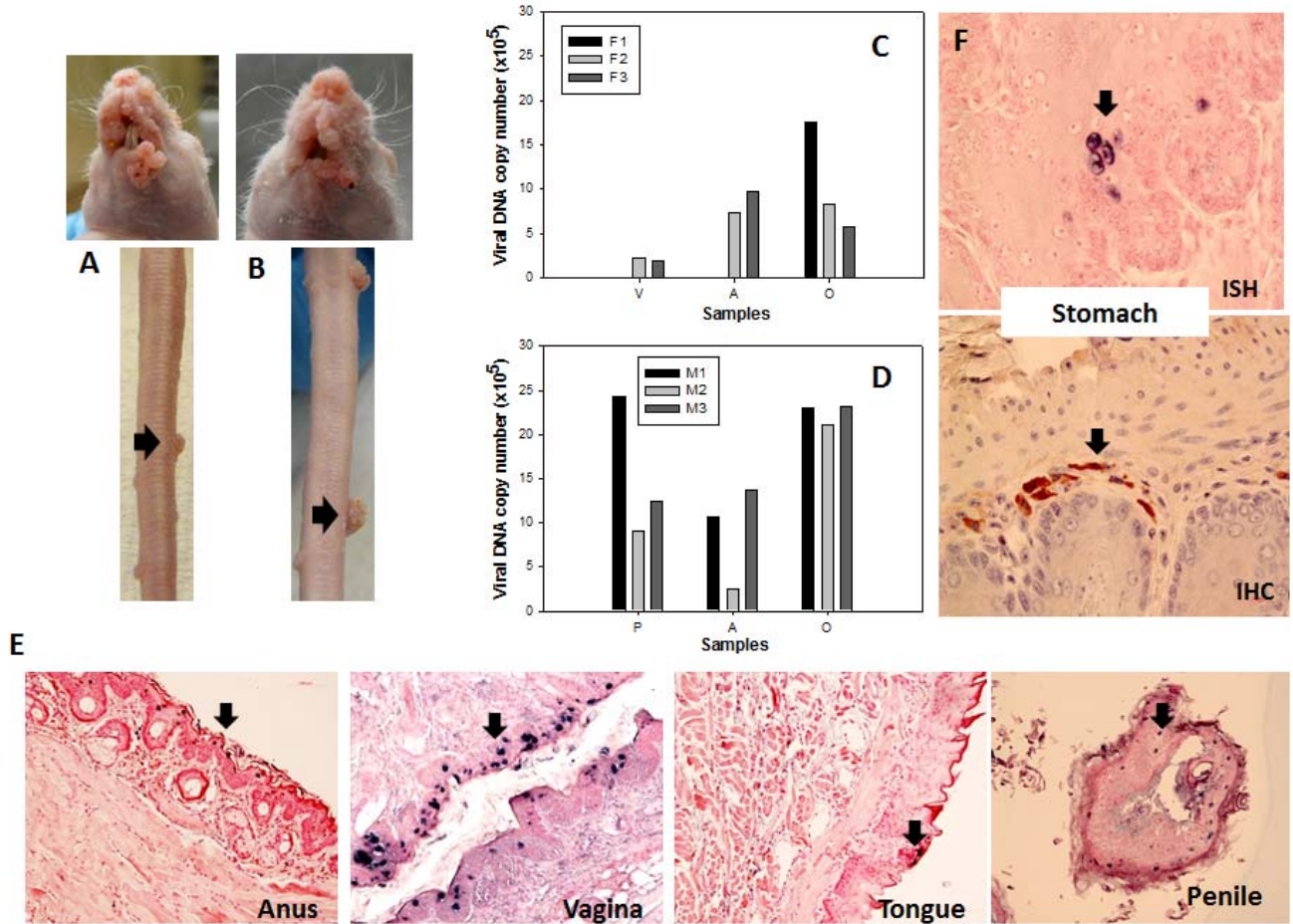
980

981

982

983 **Figure 10.**

984



985

986

987

988

989

990

991

992

993 REFERENCES

- 994 Agalliu, I., Z. Chen, T. Wang, R.B. Hayes, N.D. Freedman, S.M. Gapstur, and R.D. Burk. 2018.
995 Oral Alpha, Beta and Gamma HPV Types and Risk of Incident Esophageal Cancer.
996 *Cancer Epidemiol Biomarkers Prev*
- 997 Akhtar, N., and J.G. Bansal. 2017. Risk factors of Lung Cancer in nonsmoker. *Curr Probl*
998 *Cancer* 41:328-339.
- 999 Baandrup, L., L.T. Thomsen, T.B. Olesen, K.K. Andersen, B. Norrild, and S.K. Kjaer. 2014. The
1000 prevalence of human papillomavirus in colorectal adenomas and adenocarcinomas: a
1001 systematic review and meta-analysis. *Eur. J. Cancer* 50:1446-1461.
- 1002 Bodaghi, S., L.V. Wood, G. Roby, C. Ryder, S.M. Steinberg, and Z.M. Zheng. 2005a. Could
1003 human papillomaviruses be spread through blood? *J Clin Microbiol* 43:5428-5434.
- 1004 Bodaghi, S., K. Yamanegi, S.Y. Xiao, M. Da Costa, J.M. Palefsky, and Z.M. Zheng. 2005b.
1005 Colorectal papillomavirus infection in patients with colorectal cancer. *Clin Cancer Res*
1006 11:2862-2867.
- 1007 Bolger, A.M., M. Lohse, and B. Usadel. 2014. Trimmomatic: a flexible trimmer for Illumina
1008 sequence data. *Bioinformatics* 30:2114-2120.
- 1009 Campo, M.S. 2002. Animal models of papillomavirus pathogenesis. *Virus Res* 89:249-261.
- 1010 Chen, A.C., A. Keleher, M.A. Kedda, A.B. Spurdle, N.A. McMillan, and A. Antonsson. 2009.
1011 Human papillomavirus DNA detected in peripheral blood samples from healthy
1012 Australian male blood donors. *J Med Virol* 81:1792-1796.
- 1013 Christensen, N.D., L.R. Budgeon, N.M. Cladel, and J. Hu. 2017. Recent advances in preclinical
1014 model systems for papillomaviruses. *Virus Res* 231:108-118.
- 1015 Christensen, N.D., and J.W. Kreider. 1991. Neutralization of CRPV infectivity by monoclonal
1016 antibodies that identify conformational epitopes on intact virions. *Virus Res* 21:169-179.
- 1017 Christensen, N.D., C.A. Reed, N.M. Cladel, R. Han, and J.W. Kreider. 1996. Immunization with
1018 viruslike particles induces long-term protection of rabbits against challenge with
1019 cottontail rabbit papillomavirus. *J. Virol* 70:960-965.
- 1020 Cladel, N.M., L.R. Budgeon, K.K. Balogh, T.K. Cooper, S.A. Brendle, N.D. Christensen, T.D.
1021 Schell, and J. Hu. 2017a. Mouse papillomavirus infection persists in mucosal tissues of
1022 an immunocompetent mouse strain and progresses to cancer. *Sci Rep* 7:16932.
- 1023 Cladel, N.M., L.R. Budgeon, K.K. Balogh, T.K. Cooper, J. Hu, and N.D. Christensen. 2015. A
1024 novel pre-clinical murine model to study the life cycle and progression of cervical and
1025 anal papillomavirus infections. *PLoS One* 10:e0120128.
- 1026 Cladel, N.M., L.R. Budgeon, K.K. Balogh, T.K. Cooper, J. Hu, and N.D. Christensen. 2016.
1027 Mouse papillomavirus MmuPV1 infects oral mucosa and preferentially targets the base
1028 of the tongue. *Virology* 488:73-80.
- 1029 Cladel, N.M., L.R. Budgeon, T.K. Cooper, K.K. Balogh, N.D. Christensen, R. Myers, V.
1030 Majerciak, D. Gotte, Z.M. Zheng, and J. Hu. 2017b. Mouse papillomavirus infections
1031 spread to cutaneous sites with progression to malignancy. *J Gen Virol*
- 1032 Cladel, N.M., L.R. Budgeon, T.K. Cooper, K.K. Balogh, J. Hu, and N.D. Christensen. 2013.
1033 Secondary infections, expanded tissue tropism, and evidence for malignant potential in
1034 immunocompromised mice infected with *Mus musculus* papillomavirus 1 DNA and
1035 virus. *J. Virol* 87:9391-9395.

- 1036 Cladel, N.M., J. Hu, K. Balogh, A. Mejia, and N.D. Christensen. 2008. Wounding prior to
1037 challenge substantially improves infectivity of cottontail rabbit papillomavirus and allows
1038 for standardization of infection. *J. Virol. Methods* 148:34-39.
- 1039 Cocuzza, C.E., M. Martinelli, F. Sina, A. Piana, G. Sotgiu, T. Dell'Anna, and R. Musumeci.
1040 2017. Human papillomavirus DNA detection in plasma and cervical samples of women
1041 with a recent history of low grade or precancerous cervical dysplasia. *PLoS One*
1042 12:e0188592.
- 1043 Damin, D.C., M.B. Caetano, M.A. Rosito, G. Schwartzmann, A.S. Damin, A.P. Frazzon, R.D.
1044 Ruppenthal, and C.O. Alexandre. 2007. Evidence for an association of human
1045 papillomavirus infection and colorectal cancer. *Eur J Surg Oncol* 33:569-574.
- 1046 Dobin, A., C.A. Davis, F. Schlesinger, J. Drenkow, C. Zaleski, S. Jha, P. Batut, M. Chaisson, and
1047 T.R. Gingeras. 2013. STAR: ultrafast universal RNA-seq aligner. *Bioinformatics* 29:15-
1048 21.
- 1049 Doorbar, J. 2016. Model systems of human papillomavirus-associated disease. *J Pathol* 238:166-
1050 179.
- 1051 ElAmrani, A., T. Gheit, M. Benhessou, S. McKay-Chopin, M. Attaleb, S. Sahraoui, M. El
1052 Mzibri, M. Corbex, M. Tommasino, and M. Khyatti. 2018. Prevalence of mucosal and
1053 cutaneous human papillomavirus in Moroccan breast cancer. *Papillomavirus Res* 5:150-
1054 155.
- 1055 Escudero Duch, C., R.A. Williams, R.M. Timm, J. Perez-Tris, and L. Benitez. 2015. A Century
1056 of Shope Papillomavirus in Museum Rabbit Specimens. *PLoS One* 10:e0132172.
- 1057 Glenn, W.K., C.C. Ngan, T.G. Amos, R.J. Edwards, J. Swift, L. Lutze-Mann, F. Shang, N.J.
1058 Whitaker, and J.S. Lawson. 2017. High risk human papilloma viruses (HPVs) are present
1059 in benign prostate tissues before development of HPV associated prostate cancer. *Infect*
1060 *Agent Cancer* 12:46.
- 1061 Gravitt, P.E. 2011. The known unknowns of HPV natural history. *J Clin Invest* 121:4593-4599.
- 1062 Gravitt, P.E. 2012. Evidence and impact of human papillomavirus latency. *Open Virol J* 6:198-
1063 203.
- 1064 Gravitt, P.E., and R.L. Winer. 2017. Natural History of HPV Infection across the Lifespan: Role
1065 of Viral Latency. *Viruses* 9:
- 1066 Hu, J., L.R. Budgeon, K.K. Balogh, X. Peng, N.M. Cladel, and N.D. Christensen. 2014. Long-
1067 peptide therapeutic vaccination against CRPV-induced papillomas in HLA-A2.1
1068 transgenic rabbits. *Trials Vaccinol* 3:134-142.
- 1069 Hu, J., L.R. Budgeon, N.M. Cladel, K. Balogh, R. Myers, T.K. Cooper, and N.D. Christensen.
1070 2015. Tracking vaginal, anal and oral infection in a mouse papillomavirus infection
1071 model. *J Gen Virol* 96:3554-3565.
- 1072 Hu, J., L.R. Budgeon, N.M. Cladel, T.D. Culp, K.K. Balogh, and N.D. Christensen. 2007a.
1073 Detection of L1, infectious virions and anti-L1 antibody in domestic rabbits infected with
1074 cottontail rabbit papillomavirus. *J. Gen. Virol* 88:3286-3293.
- 1075 Hu, J., N. Cladel, K. Balogh, and N. Christensen. 2010. Mucosally delivered peptides prime
1076 strong immunity in HLA-A2.1 transgenic rabbits. *Vaccine*
- 1077 Hu, J., N.M. Cladel, K. Balogh, L. Budgeon, and N.D. Christensen. 2007b. Impact of genetic
1078 changes to the CRPV genome and their application to the study of pathogenesis in vivo.
1079 *Virology* 358:384-390.
- 1080 Hu, J., N.M. Cladel, L.R. Budgeon, K.K. Balogh, and N.D. Christensen. 2017. The Mouse
1081 Papillomavirus Infection Model. *Viruses* 9:

- 1082 Hu, J., N.M. Cladel, M.D. Pickel, and N.D. Christensen. 2002. Amino Acid residues in the
1083 carboxy-terminal region of cottontail rabbit papillomavirus e6 influence spontaneous
1084 regression of cutaneous papillomas. *J. Virol* 76:11801-11808.
- 1085 Ingle, A., S. Ghim, J. Joh, I. Chepkoech, A. Bennett Jenson, and J.P. Sundberg. 2011. Novel
1086 laboratory mouse papillomavirus (MusPV) infection. *Vet Pathol* 48:500-505.
- 1087 Jeannot, E., V. Becette, M. Campitelli, M.A. Calmejane, E. Lappartient, E. Ruff, S. Saada, A.
1088 Holmes, D. Bellet, and X. Sastre-Garau. 2016. Circulating human papillomavirus DNA
1089 detected using droplet digital PCR in the serum of patients diagnosed with early stage
1090 human papillomavirus-associated invasive carcinoma. *J Pathol Clin Res* 2:201-209.
- 1091 Khoury, R., S. Sauter, M. Butsch Kovacic, A.S. Nelson, K.C. Myers, P.A. Mehta, S.M. Davies,
1092 and S.I. Wells. 2018. Risk of Human Papillomavirus Infection in Cancer-Prone
1093 Individuals: What We Know. *Viruses* 10:
- 1094 Kreider, J.W., N.M. Cladel, S.D. Patrick, P.A. Welsh, S.L. DiAngelo, J.M. Bower, and N.D.
1095 Christensen. 1995. High efficiency induction of papillomas in vivo using recombinant
1096 cottontail rabbit papillomavirus DNA. *J. Virol. Methods* 55:233-244.
- 1097 Laffort, C., F. Le Deist, M. Favre, S. Caillat-Zucman, I. Radford-Weiss, M. Debre, S. Fraitag, S.
1098 Blanche, M. Cavazzana-Calvo, B.G. de Saint, J.P. de Villartay, S. Giliani, G. Orth, J.L.
1099 Casanova, C. Bodemer, and A. Fischer. 2004. Severe cutaneous papillomavirus disease
1100 after haemopoietic stem-cell transplantation in patients with severe combined immune
1101 deficiency caused by common gammac cytokine receptor subunit or JAK-3 deficiency.
1102 *Lancet* 363:2051-2054.
- 1103 Li, B., and C.N. Dewey. 2011. RSEM: accurate transcript quantification from RNA-Seq data
1104 with or without a reference genome. *BMC Bioinformatics* 12:323.
- 1105 Malhone, C., A. Longatto-Filho, and J.R. Filassi. 2018. Is Human Papilloma Virus Associated
1106 with Breast Cancer? A Review of the Molecular Evidence. *Acta Cytol* 62:166-177.
- 1107 Martinez, G.G., and J.N. Troconis. 2014. [Natural history of the infection for human
1108 papillomavirus: an actualization]. *Invest Clin* 55:82-91.
- 1109 Metsalu, T., and J. Vilo. 2015. ClustVis: a web tool for visualizing clustering of multivariate data
1110 using Principal Component Analysis and heatmap. *Nucleic Acids Res* 43:W566-570.
- 1111 Mirzaei, H., H. Goudarzi, G. Eslami, and E. Faghihloo. 2018. Role of viruses in gastrointestinal
1112 cancer. *J Cell Physiol* 233:4000-4014.
- 1113 Moustafa, A., C. Xie, E. Kirkness, W. Biggs, E. Wong, Y. Turpaz, K. Bloom, E. Delwart, K.E.
1114 Nelson, J.C. Venter, and A. Telenti. 2017. The blood DNA virome in 8,000 humans.
1115 *PLoS Pathog* 13:e1006292.
- 1116 Phipson, B., S. Lee, I.J. Majewski, W.S. Alexander, and G.K. Smyth. 2016. Robust
1117 Hyperparameter Estimation Protects against Hypervariable Genes and Improves Power to
1118 Detect Differential Expression. *Ann Appl Stat* 10:946-963.
- 1119 Russo, G.I., A.E. Calogero, R.A. Condorelli, G. Scalia, G. Morgia, and S. La Vignera. 2018.
1120 Human papillomavirus and risk of prostate cancer: a systematic review and meta-
1121 analysis. *Aging Male* 1-7.
- 1122 Sadeghi, M., B. Kapusinszky, D.M. Yugo, T.G. Phan, X. Deng, I. Kanevsky, T. Opriessnig, A.R.
1123 Woolums, D.J. Hurley, X.J. Meng, and E. Delwart. 2017. Virome of US bovine calf
1124 serum. *Biologicals* 46:64-67.
- 1125 Salyakina, D., and N.F. Tsinoremas. 2013. Viral expression associated with gastrointestinal
1126 adenocarcinomas in TCGA high-throughput sequencing data. *Hum Genomics* 7:23.

- 1127 Serrano, B., M. Brotons, F.X. Bosch, and L. Bruni. 2017. Epidemiology and burden of HPV-
1128 related disease. *Best Pract Res Clin Obstet Gynaecol*
- 1129 Shanis, D., P. Anandi, C. Grant, A. Bachi, N. Vyas, M.A. Merideth, P.A. Pophali, E. Koklanaris,
1130 S. Ito, B.N. Savani, A.J. Barrett, M. Battiwalla, and P. Stratton. 2018. Risks factors and
1131 timing of genital human papillomavirus (HPV) infection in female stem cell transplant
1132 survivors: a longitudinal study. *Bone Marrow Transplant* 53:78-83.
- 1133 Shew, M.L., A.C. Ermel, Y. Tong, W. Tu, B. Qadadri, and D.R. Brown. 2015. Episodic
1134 detection of human papillomavirus within a longitudinal cohort of young women. *J Med*
1135 *Viol* 87:2122-2129.
- 1136 Shigehara, K., T. Sasagawa, and M. Namiki. 2014. Human papillomavirus infection and
1137 pathogenesis in urothelial cells: a mini-review. *J Infect Chemother* 20:741-747.
- 1138 Shikova, E., Z. Ivanova, D. Alexandrova, M. Shindov, and A. Lekov. 2017. Human
1139 papillomavirus prevalence in lung carcinomas in Bulgaria. *Microbiol Immunol* 61:427-
1140 432.
- 1141 Stramer, S.L. 2014. Current perspectives in transfusion-transmitted infectious diseases: emerging
1142 and re-emerging infections. *ISBT Sci Ser* 9:30-36.
- 1143 Taberna, M., M. Mena, M.A. Pavon, L. Alemany, M.L. Gillison, and R. Mesia. 2017. Human
1144 papillomavirus-related oropharyngeal cancer. *Ann Oncol* 28:2386-2398.
- 1145 Tachezy, R., J. Hrbacek, J. Heracek, M. Salakova, J. Smahelova, V. Ludvikova, A. Svec, M.
1146 Urban, and E. Hamsikova. 2012. HPV persistence and its oncogenic role in prostate
1147 tumors. *J Med Virol* 84:1636-1645.
- 1148 Uberoi, A., and P.F. Lambert. 2017. Rodent Papillomaviruses. *Viruses* 9:
- 1149 Xiao, W., and J.L. Brandsma. 1996. High efficiency, long-term clinical expression of cottontail
1150 rabbit papillomavirus (CRPV) DNA in rabbit skin following particle-mediated DNA
1151 transfer. *Nucleic Acids Res* 24:2620-2622.
- 1152 Xue, X.Y., V. Majerciak, A. Uberoi, B.H. Kim, D. Gotte, X. Chen, M. Cam, P.F. Lambert, and
1153 Z.M. Zheng. 2017. The full transcription map of mouse papillomavirus type 1
1154 (MmuPV1) in mouse wart tissues. *PLoS Pathog* 13:e1006715.
- 1155 Zeng, Z.M., F.F. Luo, L.X. Zou, R.Q. He, D.H. Pan, X. Chen, T.T. Xie, Y.Q. Li, Z.G. Peng, and
1156 G. Chen. 2016. Human papillomavirus as a potential risk factor for gastric cancer: a
1157 meta-analysis of 1,917 cases. *Onco Targets Ther* 9:7105-7114.
- 1158
- 1159